



Cite this: *J. Mater. Chem. C*, 2025, 13, 21275

## From nature's masters of camouflage to engineered optics: cephalopod-inspired materials and technologies

Chengyi Xu  <sup>abcd</sup>

Cephalopods (e.g., octopus, squid, and cuttlefish) are a class of soft-bodied marine invertebrates renowned for their ability to dynamically alter their color and appearance for camouflage in complex environments. Despite their popularity in human history and culture, the mechanisms underlying the dazzling visual feats displayed by cephalopod skin were not fully understood until recent decades. These feats are enabled by a synchronized orchestra of thousands to millions of dynamic bio-optical components embedded in the skin, each comprising highly evolved biological structures and a unique materials foundation, capable of unparalleled manipulation of incident light through neuromuscular or biochemical control. While our fundamental understanding of cephalopod optical biology and camouflage behaviors continues to evolve, it has already inspired numerous man-made technologies over the past decade with tunable optical functionalities across various spectral ranges. However, a comprehensive and up-to-date overview covering cephalopod camouflage tactics at the animal level, the underlying mechanisms at the organ and cellular levels, and the development of dynamic optical materials and systems derived from and inspired by cephalopod skin remains lacking and is highly needed. In this review, we summarize key recent advances in the optical biology of cephalopods and discuss how these insights have informed the design of dynamic, stimuli-responsive optical materials and systems. In addition, we provide our perspectives on future research directions in this rapidly growing field, with the aim to stimulate interdisciplinary research across cephalopod biology, materials science, and engineering domains.

Received 6th June 2025,  
Accepted 8th September 2025

DOI: 10.1039/d5tc02185e

rsc.li/materials-c

### 1. Cephalopod and human history

Cephalopods are a class of marine invertebrates in the molluscan phylum. The evolution of cephalopods can be traced back to ~530 million years ago in the late Cambrian, which is widely agreed upon by paleontologists to be earlier than the first appearance of vertebrates.<sup>1</sup> After millions of years of evolution, there are over 750 cephalopod species nowadays that have been discovered and distributed in most parts of the ocean around the world, from shallow-water coastal regions to dark water columns at abyssal depths.<sup>2,3</sup> Indeed, modern cephalopods are strikingly different from species to species when evaluated with

various metrics, such as size, weight, appearance, body structure, and behavior, but in general, these animals can be categorized into two major divisions that include nautiloids and coleoids.<sup>2,3</sup> Nautiloids have only a handful of existing species, for example, *Nautilus* and *Allonautilus*, which feature rigid external shells with gas-filled chambers that are mainly used for buoyancy and protection.<sup>4,5</sup> These very few remaining species of nautiloids are known as 'living fossils', because their primitive shelled body structures highly resemble those of ancient cephalopods that went extinct quite a long time ago.<sup>4,5</sup> Coleoids constitute the majority of modern cephalopods and encompass subdivisions that include decapodiformes (eight arms and two tentacles) and octopodiformes (only eight arms), as represented by common examples such as squid, cuttlefishes, and octopuses.<sup>2,3</sup> Unlike nautiloids, coleoid cephalopods usually feature soft bodies, with rigid shells being internalized, reduced, or even completely lost during evolution.<sup>2,3</sup> Overall, cephalopods, including nautiloids and coleoids, have a high level of species diversity and play a crucial role in global marine ecosystems.

Cephalopods share close ties with human beings from historical, cultural, and scientific perspectives. Early around

<sup>a</sup> Department of Mechanical and Materials Engineering, School of Engineering, University of Alabama at Birmingham, Birmingham, AL 35294, USA.

E-mail: cxu@uab.edu

<sup>b</sup> Neuroengineering PhD Program, School of Engineering, University of Alabama at Birmingham, Birmingham, AL 35294, USA

<sup>c</sup> Graduate Biological Science Program, University of Alabama at Birmingham, Birmingham, AL 35294, USA

<sup>d</sup> Comprehensive Neuroscience Center, Heersink School of Medicine, University of Alabama at Birmingham, Birmingham, AL 35294, USA



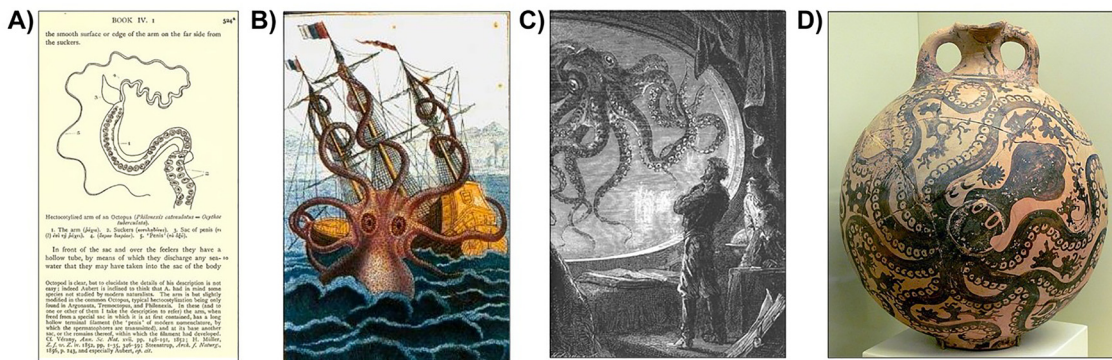


**Fig. 1** Cephalopods in Human History. (A) A lost diagram of an octopus arm in Aristotle's book "History of Animals" (c. 350 BCE).<sup>7</sup> The diagram was reconstructed by D'Arcy Thompson (1910 CE).<sup>8</sup> (B) A drawing of an imaginary colossal octopus called the *Kraken* devouring a ship by Pierre Dénys de Montfort (1801 CE).<sup>10</sup> (C) An illustration in Jules Verne's "Twenty Thousand Leagues Under the Sea" by Alphonse de Neuville and Édouard Riou (1870 CE), showing Captain Nemo viewing a giant squid from the *Nautilus* submarine.<sup>12</sup> (D) A picture of an ancient octopus-patterned vase unearthed at Palaikastro, Greece (c. 1500 BCE).<sup>13</sup> The picture was taken by Wolfgang Sauber (2009 CE). Parts A, B, and C are in the Public Domain and were reproduced via Wikimedia Commons. Part D was reproduced from an image by Wolfgang Sauber via Wikimedia Commons (Creative Commons Attribution-Share Alike 3.0).

4000 years ago, ancient Chinese described the discovery of an unusual 'ten-body' fish in a classic geographical and cultural account called "*The Classic of Mountains and Seas*".<sup>6</sup> This mysterious 'ten-body' fish was later believed to be shallow-water squid that was known to have eight arms and two tentacles.<sup>6</sup> Around 350 BCE, the Greek philosopher Aristotle described in his book "*History of Animals*" about cephalopods (Fig. 1A).<sup>7,8</sup> Aristotle observed that octopuses and sepia cuttlefishes could render their body colors to match adjacent stones in the surrounding environments for hunting purposes, and they could perform similar color-changing tricks when alarmed.<sup>7,8</sup> These two examples represented early written reports of cephalopods in human history and confirmed our ancestors' direct observation and interaction with these animals.



**Chengyi Xu**

Zhenan Bao in the Department of Chemical Engineering at Stanford University. He received his PhD in Materials Science and Engineering from the University of California, Irvine. His expertise lies in combining materials design, advanced manufacturing, and bioinspired engineering to enable next-generation interactive interfaces across humans, robots, and the environment.

*Dr Chengyi Xu is currently an Assistant Professor in the Department of Mechanical and Materials Engineering, an Affiliated Faculty member in the Neuroengineering and Graduate Biological Science Programs, and an Associate Scientist at the Comprehensive Neuroscience Center at the Heersink School of Medicine at the University of Alabama at Birmingham. Previously, he worked as a research staff scientist and postdoctoral researcher with Professor*

Indeed, cephalopods have served as inspiration sources for countless fictional mythologies and novels, such as the famous sea monster named *Kraken* in Scandinavian folklore (Fig. 1B) and the giant squid in Jules Verne's "Twenty Thousand Leagues under the Sea" (Fig. 1C).<sup>9–12</sup> In addition, cephalopods are aesthetically appealing for their marvelous body forms and appearances, and they have been continuously stimulating the creation of numerous artworks, from ancient ceramic wares, as exemplified by a delicate octopus-patterned vase that was unearthed in Palaikastro (Fig. 1D),<sup>13</sup> to paintings, as exemplified by Giuseppe Arcimboldo's "*The Allegory of Water*" from the Renaissance.<sup>14</sup> Since around a century ago, cephalopods have also started to garner growing interest within the scientific community, with an extensive amount of research performed to explore and elucidate the evolutionary,<sup>15,16</sup> physiological,<sup>17</sup> structural,<sup>18</sup> and ethological<sup>3,19</sup> properties of these marine animals, which in turn have facilitated progress in other emerging areas such as neuroscience,<sup>20</sup> bioelectronics,<sup>21</sup> and robotics.<sup>22</sup> Taken together, cephalopods have demonstrated enormous impacts on our culture and science along with human history.

## 2. Cephalopod camouflage tactics

Cephalopods are considered the most intelligent invertebrates with a high level of intelligence that is comparable to or even exceeds many vertebrate rivals.<sup>23,24</sup> During evolution, cephalopods have developed highly complex central and peripheral nervous systems, which serve as physical foundations for their intelligence, thus enabling a variety of advanced functions, such as episodic-like memory (*i.e.*, remember what occurred during an episode, where it took place, and when it happened), ability to learn from experience, ability to perform certain activities (*e.g.*, opening jars and using tools), and rapid decision-making in ever-changing marine environments.<sup>23,24</sup> Among all, the most iconic feature of cephalopods, particularly for coleoid species that include squid, octopuses, and cuttlefishes,

is their fascinating ability to change colors and perform active camouflage, which is an unparalleled feat among all living animals on this planet.<sup>2,3</sup> Indeed, active camouflage, as an evolutionary result after millions of years, is adopted by these soft-bodied animals as a primary defense mechanism to avoid themselves being detected by predators and thus increase chances of survival (note that some species are also confirmed to use camouflage for hunting or mating purposes).<sup>2,3</sup> Cephalopods showcase a large repertoire of visual tactics to blend into surrounding environments by altering their appearances, in a much faster and more dynamic fashion when compared to other famous camouflage examples of terrestrial animals, such as chameleons,<sup>25</sup> stick insects,<sup>26</sup> and moths.<sup>27</sup> To achieve effective camouflage, cephalopods are capable of manipulating their body color, pattern, transparency, contrast, and even texture.<sup>2,3</sup> Many cephalopods can also adapt to surrounding lighting conditions by modulating the emission of light from their bodies through symbiotic relationships with bioluminescent bacteria.<sup>2,3</sup> Besides, some cephalopods are known to mimic appearances, postures, and behaviors of other extra-specific marine animals such as flatfishes and sea snakes.<sup>2,3</sup> Because there are ~750 cephalopod species and they may vary significantly from species to species, it is nearly impossible to enumerate what is possible for each single species. Instead, in this part, we will emphasize a more general discussion on various types of camouflage mechanisms, along with detailed examples of a few representative species.

## 2.1 Coloration and patterning modulation

The most common feature of cephalopods is their unmatched ability to change skin coloration and patterning.<sup>2,3</sup> As an essential tactic for camouflage and communication, adaptive color modulation in the skin has been observed and confirmed for almost all coleoid cephalopods (with only very few exceptions of deep-sea species that live at light-impenetrable depths), as exemplified by a swimming pencil squid (*Loliginidae*) reversibly changing color in front of rocks above the seafloor.<sup>28</sup> These animals are capable of generating a variety of global body patterns, which are built upon the synchronous functions of thousands to millions of tiny individual light-interacting organs and cells in the skin.<sup>3,29-37</sup> Based on previous observational studies, cephalopods' camouflage patterns can be generalized into three main categories, *i.e.*, uniform, mottled, and disruptive (Fig. 2A(i)–(iii)).<sup>3,38-40</sup> Uniform patterning features the dominant use of single colors throughout the body to resemble similar single-colored (usually bland) backgrounds, as shown by a beige-colored European common cuttlefish (*Sepia officinalis*) matching its appearance to the sandy floor (Fig. 2A(i)).<sup>40</sup> Mottled patterning features the use of relatively small-sized patches in light and dark colors that are randomly distributed across the skin to match speckled backgrounds, as shown by the same cuttlefish changing its appearance to match a different background with gravels and small pebbles (Fig. 2A(ii)).<sup>40</sup> Disruptive patterning features the display of sharply contrasting colors in relatively large-sized regions in the skin to make the body outline less conspicuous, as shown by the same cuttlefish adapting its appearance above a new

background with large pebbles (Fig. 2A(iii)).<sup>40</sup> These three basic patterns (plus many variants) can be dynamically switched under direct neural control, which allows cephalopods to quickly match almost any background within a second and thus effectively hide in complex environments.<sup>3</sup>

Besides camouflage, many cephalopods also use dynamic body patterning for a variety of other purposes, such as secondary defense mechanism, communication, and signaling.<sup>3,36</sup> As one example, in cases where the primary defense mechanism (*i.e.*, camouflage) fails, an Atlantic white-spotted octopus (*Callistoctopus macropus*) can suddenly change its body appearance into a high-contrast reddish pattern with sparsely distributed white spots (Fig. 2A(iv)).<sup>41</sup> This dramatic deimatic display, as commonly seen in various animals, is effective to startle the predators and thus gain the octopus more time to expel ink and escape.<sup>42</sup> As another example, a male Caribbean reef squid (*Sepioteuthis sepioides*) can split its body pattern into two strikingly different halves, with the right half appearing dark brown to attract a female squid and the left half appearing silvery-white to repel rival males (Fig. 2A(v)).<sup>43</sup> Note that the half-bodied pattern can be rapidly flipped in seconds. As a third example, flamboyant cuttlefishes (*Metasepia pfefferi*) are famous for their vivid coloration with a series of pigmentary black stripes constantly moving across the body, which are known as 'passing clouds' (Fig. 2A(vi)).<sup>44</sup> These eye-catching flashing patterns can send out warning (poisonous) signals to confuse or dismay potential predators, although, interestingly, the *M. pfefferi* cuttlefishes only produce neurotoxins at trace amounts. Altogether, these examples readily showcase cephalopods' versatile abilities to change color and patterning under various circumstances.

## 2.2 Transparency modulation

Transparency modulation is another tactic that is frequently performed by many cephalopods to hide from the detection of predators. Such transparency-modulating cephalopod species, as exemplified by mesopelagic octopuses (*Japetella heathi*) (Fig. 2B(i))<sup>45</sup> and glass squid (*Taonius borealis*) (Fig. 2B(ii)),<sup>46,47</sup> are usually found in the deep ocean (600–1000 m), where only two sources of light are available: (1) extremely weak downwelling light from the ocean's surface, and (2) bioluminescence. As one example, a *J. heathi* octopus can achieve active camouflage in somewhat featureless water columns by dynamically adjusting the transmission of light and switching between a highly transparent state and a highly opaque (pigmentary) state (Fig. 2B(i)).<sup>45</sup> In the transparent state, the *J. heathi* octopus allows the very weak downwelling light to directly pass through its nearly transparent body, which largely minimizes the overall silhouette when viewed from below in the same water column, thus making the octopus invisible to many deep-sea predators that rely on the variation of downwelling light and silhouette to forage (Fig. 2B(i) left).<sup>45</sup> However, it is noted that being transparent does not protect the *J. heathi* octopus from a specific group of predators that have evolved with bioluminescence headlights (usually in blue color), because the non-ideally transparent body of the *J. heathi* octopus inevitably scatters a fraction of light upon bioluminescence illumination, making it



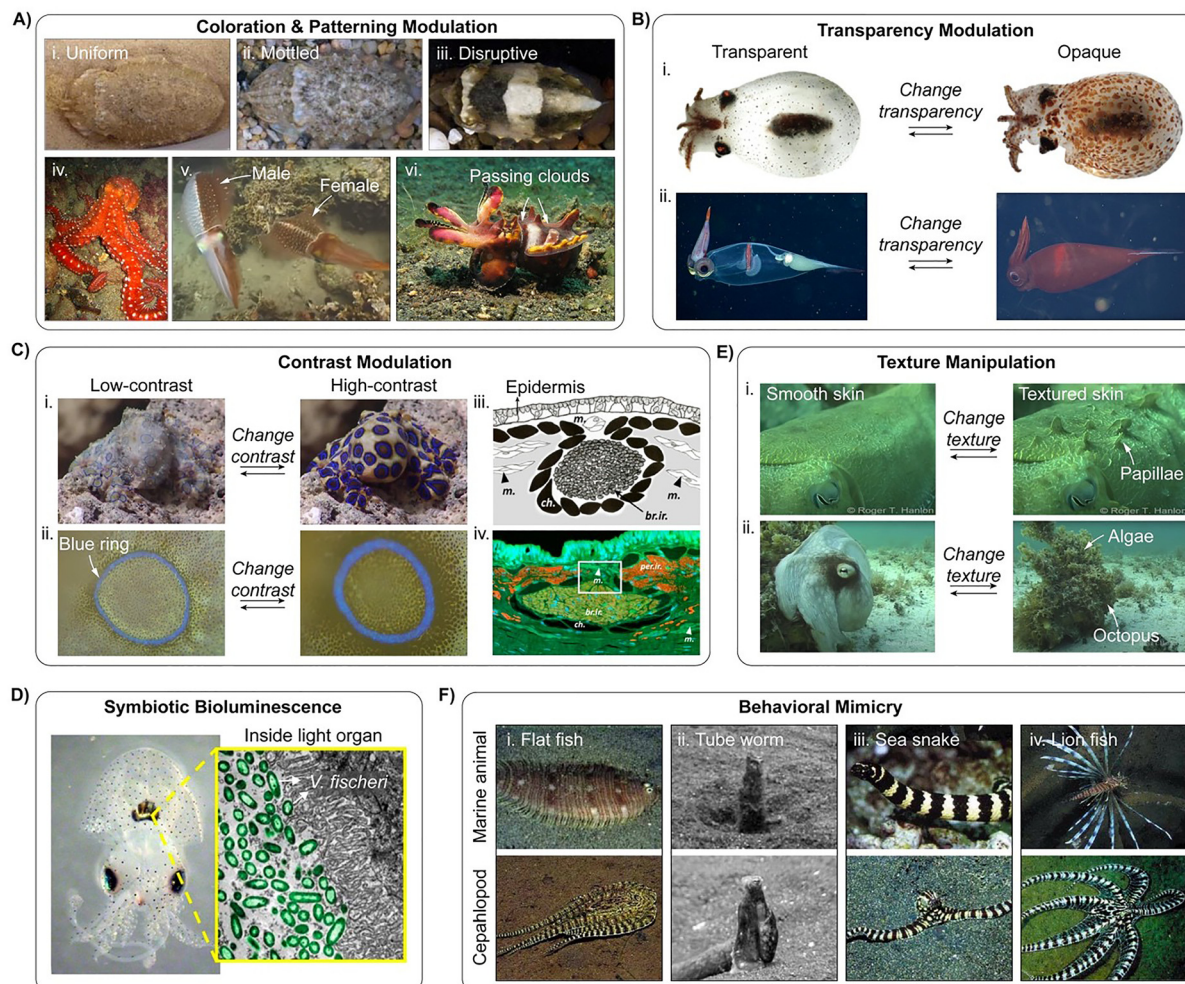


**Fig. 2** Cephalopod camouflage tactics at the animal level. (A) Color and patterning modulation. An *S. officinalis* cuttlefish adapting its body appearance to match different backgrounds, with the skin pattern changing from (i) uniform to (ii) mottled to (iii) disruptive.<sup>40</sup> (iv) An Atlantic white-spotted octopus (*Callistoctopus macropus*) displaying a deimatic reddish pattern with sparsely distributed white spots.<sup>41</sup> (v) A male Caribbean reef squid (*Sepioteuthis sepioidea*) splitting its body pattern into two different halves to attract a female squid during mating activities.<sup>43</sup> (vi) A flamboyant cuttlefish (*Metasepia pfefferi*) showing vivid skin coloration with constantly moving pigmentary stripes (known as passing clouds) on the dorsal side of the mantle.<sup>44</sup> (B) Transparency modulation. (i) Pictures of a representative mesopelagic octopus (*Japetella heathi*) reversibly switching its body appearance between transparent and opaque states.<sup>46</sup> (ii) Pictures of a representative glass squid (*Taonius borealis*) reversibly switching its body appearance between transparent and opaque states.<sup>46,47</sup> (C) Contrast modulation. (i) Images of a blue-ringed octopus (*Hapalochlaena lunulata*) flashing blue rings and switching the body appearance from a low-contrast state (left) to a high-contrast state (right).<sup>48</sup> (ii) Close-up images of an individual blue ring in the same octopus' skin switching from a low-contrast state (left) to a high-contrast state (right).<sup>48</sup> (iii) A schematic of the cross-sectional architecture of a blue ring, showing the arrangement of bright iridophores in the blue ring (br.ir.), surrounding chromatophore organs (ch.), and proximal muscles (m.). (iv) A confocal microscopy image of the cross-sectional architecture of a blue ring.<sup>49</sup> (D) Symbiotic bioluminescence. A digital camera image of another *Euprymna scolopes* squid. The inset shows that bioluminescent bacteria (*Vibrio fischeri*) occupy and live inside a light organ that is located in the squid mantle.<sup>51</sup> Note that the bioluminescent bacteria were colored in green for visualization. (E) Texture manipulation. (i) Images of an Australian giant cuttlefish (*Sepia apama*) reversibly changing its skin texture.<sup>55</sup> Note that papillae can be expressed to form a highly textured skin surface. The images were taken by Roger Hanlon and reproduced with permission. (ii) Images of a common octopus (*Octopus vulgaris*) reversibly changing its skin texture and appearance.<sup>37</sup> Note that the octopus can perform realistic 3D camouflage and perfectly blend itself into the undulating algae above the seafloor. (F) Behavioral Mimicry. (i) A mimic octopus swimming across the seafloor (bottom), mimicking the typical appearance and motion of a flatfish (top).<sup>61</sup> (ii) A mimic octopus sitting still on the seafloor (bottom), resembling the typical posture of a sessile tube worm (top).<sup>62</sup> (iii) A mimic octopus buried itself in a sand burrow with two long black-and-white banded arms undulating outside (bottom), mimicking the shape, pattern, and movement of a typical sea snake (top).<sup>61</sup> (iv) A mimic octopus moving above the seafloor with all eight arms extended (bottom), resembling the typical body form of a lionfish (top).<sup>61</sup> The images in Part A (i)–(iii) were reproduced with permission from Springer Nature (Copyright © 2009). The image in Part A (iv) was taken by the SJBnormali Team and reproduced under the Creative Commons Attribution-Share Alike 3.0 Unported license via Wikimedia Commons. The image in Part A (v) was taken by Roger Hanlon and reproduced with permission. The image in Part A (vi) was taken by Silke Baron and reproduced under the Creative Commons Attribution 2.0 Generic license via Wikimedia Commons. The images in Part B (i) were reproduced with permission from Elsevier Ltd. (Copyright © 2011). The images in Part B (ii) were obtained and reproduced with permission from the Monterey Bay Aquarium Research Institute. The images in Part C (i) and (ii) were reproduced with permission from New Atlantis WILD – YouTube under the Creative Commons Attribution (CC BY) license. The images in Part C (iii) and (iv) were reproduced with permission from The Company of Biologists Ltd (Copyright © 2012). The images in Part D (i) and (ii) were taken by Roger Hanlon and reproduced with permission from Elsevier Ltd (Copyright © 2007). The images in Part E were taken by Eric Stabb and reproduced with permission. The images in Part F (i), (iii) and (iv) were taken by Mark Norman and Roger Steene and reproduced with permission from the Royal Society (Copyright © 2001), and the images in Part F (ii) were taken by Roger Hanlon and reproduced with permission from John Wiley and Sons (Copyright © 2007).



appear bright in the dark and visually distinguishable from the surrounding environment. Therefore, the highly opaque (pigmentary) state comes into play, where the skin of the *J. heathi* octopus becomes predominantly covered with much expanded pigment-containing chromatophore organs that could not be seen in the transparent state (Fig. 2B(i), right).<sup>45</sup> These expanded skin-bound chromatophores are in red or black, with very strong absorption and weak scattering of the blue-colored bioluminescence, thus making the *J. heathi* octopus appear much less conspicuous to those predators that rely on bioluminescence to forage. Notably, the *J. heathi* octopus can dynamically, reversibly, and rapidly modulate its body appearance under direct neural control and take on different transparency states in response to various lighting conditions in the environment.<sup>45</sup> Overall, transparency modulation represents an effective approach for dynamic camouflage among deep-sea cephalopods.

### 2.3. Contrast modulation

Another fascinating tactic for cephalopods to perform camouflage feats is through contrast modulation. Many coastal cephalopods are capable of manipulating their skin color contrast to match the color intensity and brightness of often complex marine environments.<sup>2,3</sup> However, in terms of contrast modulation, there may not be any examples as amazing as octopuses in the genus of *Hapalochlaena* that include blue-ringed octopuses (*Hapalochlaena lunulata*) and blue-lined octopuses (*Hapalochlaena fasciata*). As one example, an *H. lunulata* octopus can dramatically alter the color contrast of its body by flashing blue rings in the skin (Fig. 2C(i)).<sup>48</sup> When at rest, the octopus adopts a relatively low-contrast appearance with hardly noticeable ring-like patterns and thus blends perfectly into the background (Fig. 2C(i), left), but when disturbed, the same octopus can instantaneously switch to a highly conspicuous appearance with a drastically increased color contrast that now features vibrant blue rings and dark brown surrounding regions (Fig. 2C(i), right).<sup>48</sup> Indeed, the *H. lunulata* octopuses have evolved a unique actuation mechanism, along with distinct skin architectures known as blue rings (Fig. 2C(ii)), specifically for color contrast modulation, which are different from almost all other known cephalopod species.<sup>49</sup> Each individual blue ring is a miniaturized bio-optical system comprised of highly reflective iridophore cells, pigment-containing chromatophore organs, and proximal muscles (Fig. 2C(iii) and (iv)).<sup>49</sup> The iridophores, which make up the interior of the rings, function as biological Bragg stacks that reflect narrowband blue-green light and are arranged to ensure visibility of their bright iridescence over a broad range of viewing angles (Fig. 2C(iii) and (iv)).<sup>49</sup> The chromatophores, which are located beneath and around the rings, provide a pigmented dark brown background and are arranged to enhance the overall color contrast (Fig. 2C(iii) and (iv)).<sup>49</sup> The muscles, which are found on top of and around the periphery of the rings, cover the blue-green iridescence by contracting (top muscles) and relaxing (peripheral muscles) in tandem or expose the blue-green iridescence by relaxing (top muscles) and contracting (peripheral muscles) in tandem (Fig. 2C(iii) and (iv)).<sup>49</sup> Notably, hundreds of blue rings can be simultaneously activated by this neuromuscularly controlled process within only hundreds

of milliseconds, which enables the *H. lunulata* octopus' skin to rapidly flash between different contrast states (Fig. 2C(i) and (ii)).<sup>48</sup>

### 2.4. Symbiotic bioluminescence

Symbiotic bioluminescence is a distinct approach adopted by some cephalopod species for adaptive camouflage. Unlike other skin-enabled visual camouflage mechanisms, the function of symbiotic bioluminescence necessitates the involvement of a third party that can produce light, usually bioluminescent bacteria that are abundant in the ocean, to match complex lighting conditions in the marine environment. This camouflage mechanism is also known as counter-illumination, as exemplified by firefly squid (*Watasenia scintillans*), Hawaiian bobtail squid (*Euprymna scolopes*), and hummingbird bobtail squid (*Euprymna berryi*).<sup>50</sup> As one example, the *E. scolopes* squid cannot produce light by itself, instead, it shares a symbiosis relationship with bioluminescent bacteria (*Vibrio fischeri*), which colonize and live inside specialized light organs that are located in the squid skin (Fig. 2D).<sup>51-53</sup> When the sky turns dark at night, the *V. fischeri* bacteria automatically start to glow with blue/green-colored bioluminescence through a luciferin/luciferase-mediated biochemical reaction.<sup>3,52,53</sup> Then, the emitted light is reflected by a collection of well-arranged reflective tissues inside the light organs that are mainly made of high-refractive-index protein platelets.<sup>3,52,53</sup> Subsequently, the reflected light travels out of the ventral surface of the *E. scolopes* squid in a downward direction, which essentially emulates the downwelling moonlight and starlight that you would expect from a clear night sky.<sup>3,52,53</sup> In this way, the *E. scolopes* squid can effectively soften and minimize the shadow of its body and thus deceive potential predators that are located at greater depths of the same water column. Moreover, the *E. scolopes* squid demonstrates the ability to sense the environmental lighting condition and then autonomously adjust the intensity and frequency of the bioluminescence emitted from the bacteria to achieve better camouflage.<sup>3,52,53</sup> In addition, it is notable that this symbiotic mechanism between the *E. scolopes* squid and the *V. fischeri* bacteria has been extensively explored and served as a simple model system for the study of natural mutualistic symbiosis.<sup>54</sup> Overall, cephalopods showcase a delicate and beautiful camouflage mechanism through symbiotic relationships with bioluminescent bacteria.

### 2.5. Texture manipulation

While all the aforementioned camouflage mechanisms are enabled by dynamic optical interaction between the incident light and bio-optical components in the skin, the ability of cephalopods to manipulate skin textures allows them to accomplish precise and visually realize three-dimensional (3D) camouflage *via* a mechanical approach, as exemplified by many shallow-water species such as Australian giant cuttlefishes (*Sepia apama*) and common octopuses (*Octopus vulgaris*) (Fig. 2E).<sup>37,55</sup> These shallow-water cephalopods are adept at mimicking the shapes and textures of a variety of objects in their surrounding environments (e.g., rocks, coral reefs, seaweeds, and seafloors). In general, the elaborate shape-shifting behaviors of



cephalopods are enabled by neurally controlled mechanical actuation of their skin musculatures (usually muscular hydrostats) to form different types of dermal protuberances called papillae.<sup>56–58</sup> As one example, an *S. apama* cuttlefish can express individual papillae through surface buckling within a second in response to external stimuli, featuring a drastic change from smooth skin before activation (Fig. 2E(i), left) to rather rough skin after activation (Fig. 2E(i), right).<sup>55</sup> These papillae can be maintained in the extended position for over one hour *via* a unique ‘catch-like’ mechanism, without the necessity of continuous neural input, which represents a sophisticated biomechanical strategy to reduce energy cost that is usually associated with long-term camouflage.<sup>59</sup> As another example, an *O. vulgaris* octopus is able to transform its body into an algae-like form, with the bumpy papillae to resemble the algae texture and the pigmentary dark skin to match the algae coloration, perfectly blending itself into these natural algae undulating above the seafloor (Fig. 2E(ii), left).<sup>37</sup> After being disturbed by the scuba diver, it reconfigures its body, now with much smoother skin and more conspicuous bright color, and immediately jets away (Fig. 2E(ii), right).<sup>37</sup> Indeed, rapid texture modulation, along with color change, is routinely performed by these bottom-dwelling octopuses (over 150 times per hour observed for a day octopus (*Octopus cyanea*)) when out for foraging on a daily basis.<sup>2</sup> Taken together, cephalopods demonstrate unparalleled abilities of texture manipulation through mechanical actuation of skin musculatures to enable background resemblance and achieve advanced 3D camouflage.

## 2.6. Behavioral mimicry

Some cephalopod species have evolved an advanced camouflage mechanism that is known as behavioral mimicry. These masters of masquerade can not only imitate inanimate objects (described in Section 2.5) but also mimic appearances and characteristic behaviors of other extra-specific animals. Such cephalopod species are usually found on featureless sandy sea floors, as exemplified by wunderpus octopuses (*Wunderpus photogenicus*) and mimic octopuses (*Thaumoctopus mimicus*).<sup>60</sup> As one example, a *T. mimicus* octopus is capable of mimicking the behaviors of up to 13 different types of marine animals (mobile and sessile) or organisms that are locally present in its natural habitat, including flatfishes, sea snakes, lionfishes, stingrays, eels, and jellyfishes (Fig. 2F(i)–(iv)).<sup>61,62</sup> When moving fast across the open sand plain, the *T. mimicus* octopus can swim like flatfishes by matching its motion, speed, and duration, as well as displaying a flatfish-like mottled body appearance (Fig. 2F(i)).<sup>61,62</sup> When sitting still on the sand plain, the *T. mimicus* octopus can impersonate sessile invertebrates, such as sponges, tunicates, and tube worms, by reshaping its malleable body to hold a relative static posture for a long time (Fig. 2F(ii)).<sup>61,62</sup> When disturbed by small damselfishes, the *T. mimicus* octopus can bury its body into a sand burrow and leave only two long black-and-white banded arms undulating outside the burrow, which highly resembles the shape, pattern, and movement of typical sea snakes (known to prey on small damselfishes) (Fig. 2F(iii)).<sup>61,62</sup> In addition, more observational

studies have reported that *T. mimicus* octopuses can take on different mimicry forms during different activities in different environments, allowing the octopuses to remain camouflaged or unrecognized by potential predators.<sup>61,62</sup> However, to date, there is still no clear experimental or quantitative evidence to determine whether this behavioral intelligence of the *T. mimicus* octopuses is intrinsic or learned from experience over time, although it has been widely speculated to be a result of both.<sup>63</sup> Overall, versatile behavioral mimicry, together with other visual camouflage mechanisms, readily makes cephalopods the best example of camouflage in nature.

## 3. Cephalopod color-changing skin at cellular levels

Cephalopods are known as masters of disguise that have evolved with a large repertoire of visual tactics to dynamically alter coloration, appearance, and behavior for camouflage and signaling purposes. These stunning visual feats are performed across an extended surface area that covers the whole body, which are directly enabled by the synergistic function of thousands to millions of tiny constituent bio-optical and biomechanical components in the skin. In general, the architecture of cephalopod skin is highly evolved and quite sophisticated at the cellular level, which is often composed of several well-arranged organs and cells, including pigment-rich organs like chromatophores, reflective cells like iridophores and leucophores, light-emitting photophores (also known as light organs), and muscles.<sup>3,64</sup> Because of our scope and interest in this review, we will give an expanded discussion exclusively on the structure, function, and mechanism of chromatophores, iridophores, and leucophores, which represent three major types of organs and cells that have been extensively studied for their dynamic interaction with light.<sup>3,64</sup> We note that the presence, distribution, and functionality of these three types of organs and cells may vary among cephalopod species, and that our understanding of these bio-optical components is constantly evolving given the complexity of cephalopod skin.

### 3.1. Pigment-rich chromatophores

Chromatophore organs are the major optically active components in cephalopod skin that are responsible for the dominant pigmentary coloration of the whole body. These color-changing organs can be found in most parts of the body, such as mantles, fins, arms, tentacles (for squid and cuttlefishes), and near eyes (Fig. 3A).<sup>3,31,65,66</sup> They constitute the topmost chromatic layer under the epidermis and are situated above the underlying light-reflecting cells (*i.e.*, iridophores and leucophores).<sup>64</sup> Chromatophores can display multiple dark and light colors dictated by constituent pigments, including yellow, orange, pink, red, brown, and black, which are mostly located in the long-wavelength visible region of the electromagnetic spectrum.<sup>3,29–31</sup> Many coastal cephalopod species have no fewer than three types of color pigments in their chromatophores, due to their adaption to complex shallow-water habitats, while some

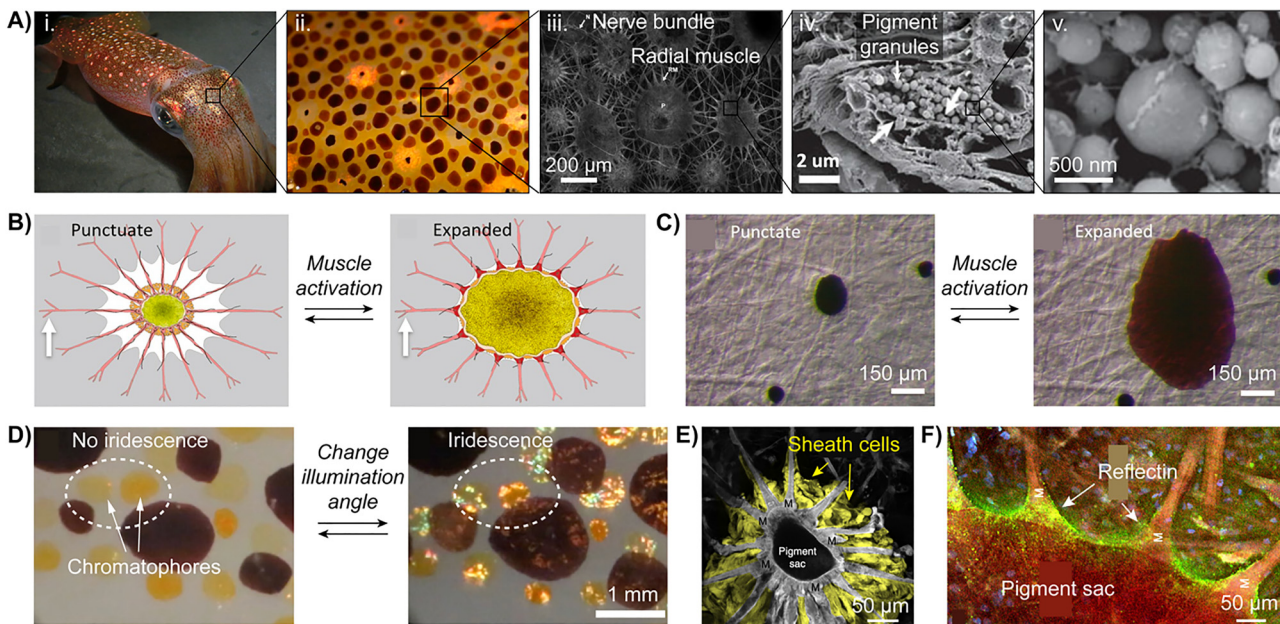


**Fig. 3** Pigment-Rich Chromatophore Organs in Cephalopod Skin. (A) Chromatophore organs at different length scales (from left to right): (i) a digital camera image of a longfin inshore squid (*Doryteuthis pealeii*).<sup>65</sup> The image was taken by Paloma T. Gonzalez-Bellido; (ii) a close-up image of the skin of a *D. pealeii* squid, showing a dense distribution of pigmentary chromatophores (dark colored spots).<sup>66</sup> The image was taken by Minette Layne; (iii) a confocal microscope image of chromatophore organs, showing radial muscles and nerve bundles connected to the central elastic pigment-containing sacculus (P) of each individual chromatophore;<sup>70</sup> (iv) a scanning electron microscope (SEM) image of the cross section of a chromatophore;<sup>68</sup> (v) a close-up SEM image of closely packed pigment granules inside the same chromatophore.<sup>68</sup> (B) A schematic of the reversible actuation of a chromatophore under direct neural control, showing a clear change in the areal coverage upon activation.<sup>71</sup> (C) Optical microscopy images of the reversible actuation of a chromatophore in the skin of a *D. pealeii* squid, showing visible changes in both the areal coverage and pigmentary coloration upon activation.<sup>71</sup> (D) Iridescence was seen in expanded chromatophores by changing the light illumination angle.<sup>73</sup> (E) Autofluorescence confocal image of a chromatophore with the sheath cells highlighted in yellow.<sup>73</sup> The pigment sac and muscle fibers (M) are enveloped by the sheath cells. (F) Confocal image of the sheath cell region showing abundant reflectin distribution inside, highlighted using a secondary antibody in green.<sup>73</sup> The image in Part A (i) was reproduced with permission from the Company of Biologists Ltd. (Copyright © 2014). The image in Part A (ii) was reproduced under the Creative Commons Attribution 2.0 Generic license via Wikimedia Commons. The image in Part A (iii) was reproduced with permission from John Wiley and Sons (Copyright © 2013). The images in Part A (iv) and (v) were reproduced with permission from the Royal Society (Copyright © 2014). The images in Parts B and C were reproduced with permission from John Wiley and Sons (Copyright © 2013). The images in Parts D–F were reproduced with permission from Springer Nature (Copyright © 2019).

deep-sea species only have one type, due to extreme dim lighting conditions at depths.<sup>3</sup> The size of chromatophores varies significantly among different species, as evaluated by the diameter in their fully expanded states, from a few hundred microns ( $\sim 300$   $\mu\text{m}$  for *Sepia officinalis* cuttlefishes) to several millimeters ( $> 1.5$  mm for *Doryteuthis pealeii* squid).<sup>3,31</sup> Dark-colored chromatophores (e.g., black and brown) usually have relatively larger sizes, and light-colored ones (e.g., yellow and red) have relatively smaller sizes.<sup>3</sup> In addition, the population of chromatophores in cephalopods differs from species to species, for example, a few hundred for some pelagic squid species and millions for many coastal cephalopod species such as *S. officinalis* and *O. vulgaris*.<sup>3</sup>

The optically active component of a chromatophore organ is chromatocyte, which consists of a central cytoelastic sacculus that encompasses packed pigment granules with diameters of hundreds of nanometers and varied sub-granular ultrastructures (Fig. 3A).<sup>67–70</sup> A set of wedge-shaped radial muscles (15–25) are attached and anchored onto the highly deformable

pigment-containing sacculus (Fig. 3A(iii)).<sup>3,31,67,71</sup> Because cephalopod skin is highly innervated with nerve bundles, these radial muscles are subject to direct neural control from the central nervous system without the involvement of any synapse (Fig. 3A(iii)).<sup>3,31,67,71</sup> At the resting state, the radial muscles are relaxed, and the sacculus is retracted into a tiny dot with the internal pigmentary granules closely packed in a small volume (Fig. 3B, left and Fig. 3C, left).<sup>71</sup> Therefore, more light is allowed to transmit through the skin, and less is absorbed. At the activated state, the radial muscles are contracted, and the sacculus is radially pulled and expanded into a much larger area with the internal pigment granules spread out in a relatively sparse distribution (Fig. 3B, right and Fig. 3C, right).<sup>71</sup> Therefore, less light is allowed to transmit through the skin, and more is absorbed. The size of the elastic pigment-containing sacculus can dramatically change upon activation, up to over 100 times, thus enabling a remarkable visible change in the overall pigmentary coloration.<sup>31</sup> Note that this neuromuscular control of chromatophore organs in cephalopod skin is quite different from the function mechanism of common

chromatophore cells found in fishes and reptiles, where pigmentary coloration is modulated by forming pigment aggregation/dispersion upon hormonal stimuli.<sup>72</sup> In comparison, one obvious advantage of direct neuromuscular control is the rapid response of chromatophores, which can be instantly activated or deactivated within only hundreds of milliseconds.<sup>3,31,71</sup> As a result, cephalopods are capable of changing color multiple times within only a few seconds, and thousands of chromatophores can be synchronously switched on and off in multiplexed formats to generate a variety of complex global patterns for dynamic camouflage in real time.

In a recent study, structural coloration was found in chromatophores in their expanded states, with iridescent patterns located precisely across the surfaces of all chromatophore color types (yellow, red, and brown) in both living squid and excised skin samples (Fig. 3D).<sup>73</sup> These patterns are visible from specific view angles between 20° and 50°. For decades, such iridescence was mistakenly attributed to the underlying structurally colored iridophores; however, it has now been confirmed to originate from the sheath cells that envelope the chromatocytes.<sup>73</sup> Within the sheath cells, reflectin protein aggregates were dispersed as small granule vesicles in a disordered fashion (Fig. 3E and F). According to a simplified optical model, one potential mechanism for this structural coloration might arise from multilayered structures between the sheath cell membranes and the thickness-tunable cytoplasm layers, which may further explain the observed color shifts upon chromatophore expansion.

### 3.2. Light-reflecting iridophores

Iridophores are a type of light-reflecting cell that accounts for the bright iridescence observed in cephalopod skin. These reflective

cells are found in different regions on the body surface that include mantles, fins, heads, and arms (Fig. 4A).<sup>3,32,74</sup> They are usually situated below the top layer of chromatophore organs and above the bottom layer of leucophore cells.<sup>64</sup> The size of iridophores varies from species to species and is usually below 1 mm.<sup>3,30</sup> Unlike pigmentary colors produced by chromatophores, most iridophores are known to display vibrant structural colors that are mostly located in the short-wavelength visible region of the electromagnetic spectrum, including blue, green, and violet, although a few exceptions of red and orange were observed in some cephalopod species.<sup>3,29,32,75,76</sup> Iridophores do not contain any color pigments, instead, they possess highly invaginated (or folded) surface morphologies that are composed of alternating micro-/nano-structures (Fig. 4A(iii)–(v)).<sup>77</sup> These multilayered structures feature periodic arrangements of membrane-enclosed proteinaceous platelets with a relatively high refractive index (mostly made of reflectin proteins) and extracellular space with a relatively low refractive index (mostly made of extracellular fluid), which essentially resembles the typical stacked configuration of a distributed Bragg reflector (Fig. 4A(v)).<sup>77</sup> Therefore, iridophores can reflect narrowband light at specific wavelengths due to constructive interference and produce angle-dependent bright iridescence on the surface.

In most cephalopod species, iridophores are found to be physiologically static, *i.e.*, their optical functionality is not responsive to external stimuli. However, there are exceptions in a few species, such as longfin inshore squid (*Doryteuthis pealeii*), where iridophores have been confirmed to exhibit tunable coloration.<sup>78</sup> Experiments have demonstrated that these dynamic iridophores are often connected or terminated with nerve fibers, which indicates that the observed tunable iridescences are related to neurally mediated processes (Fig. 4B).<sup>78</sup> The application of a

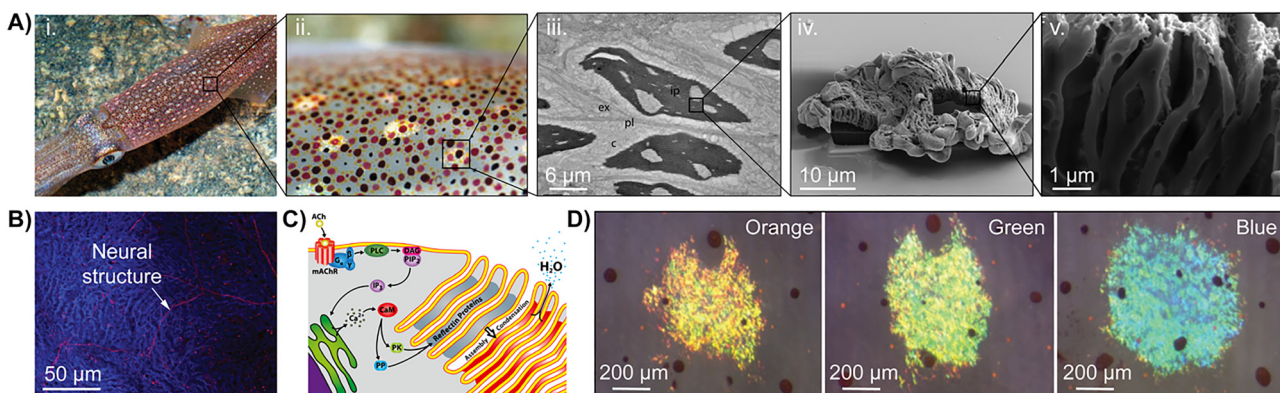


**Fig. 4** Light-Reflecting Iridophore Cells in Cephalopod Skin. (A) Iridophore cells at different length scales (from left to right): (i) a digital camera image of a longfin inshore squid (*Doryteuthis pealeii*).<sup>74</sup> (ii) a close-up image of the skin of a *D. pealeii* squid, showing sparsely distributed light-reflecting iridophore cells (bright spots).<sup>74</sup> (iii) A cross-sectional transmission electron microscope (TEM) image of several iridophore cells from a different inshore squid (*Doryteuthis opalescens*);<sup>77</sup> (iv) an SEM image of a portion of an iridophore from a *D. opalescens* squid;<sup>73</sup> (v) a close-up SEM image of the surface of the same iridophore, showing a periodic arrangement of highly invaginated structures.<sup>77</sup> (B) A confocal maximum-intensity projection image of fine neural structures (in red color) within an iridophore, confirming that iridophores are innervated.<sup>78</sup> (C) An illustration of a proposed biochemical signaling cascade process that may contribute to iridophores' tunable iridescence in response to acetylcholine (ACh).<sup>77</sup> (D) Optical microscopy images of single iridophores in the skin of a *D. pealeii* squid displaying neurally tunable structure coloration from orange (left) to green (middle) to blue (right) in response to stimuli.<sup>78</sup> The images in Part A (i) and (ii) were taken by Grayson Hanlon and reproduced with permission. The images in Part A (iii)–(v) and Part C were reproduced with permission from the National Academy of Sciences (Copyright © 2013). Part B and D were reproduced with permission from the Royal Society (Copyright © 2012).



neurotransmitter acetylcholine (ACh) triggers a biochemical signaling cascade process within the iridophore cells, initiating the phosphorylation of the constituent reflectin proteins in the alternating proteinaceous platelets and this neutralizing the initially cationic reflectin, leading to water outflux across the cell membrane (Fig. 4C).<sup>77</sup> The resulting condensation of the proteinaceous platelets causes changes in the overall geometry, refractive index, and arrangement of the Bragg-reflector-like structures on the iridophore surface (Fig. 4C).<sup>77</sup> Therefore, the iridophores can shift their reflectance peaks (*i.e.*, colors) across a broad wavelength range within the visible region of the electromagnetic spectrum (Fig. 4D).<sup>78</sup> Furthermore, the semi-permeable membrane that envelops the Bragg lamellae is thought to functionally serve as an “impedance-matched” amplifier to the stimuli-responsive reflectin assembly size.<sup>79</sup> The response time of these tunable iridophores is usually between a few seconds and a few minutes, much slower compared to that of chromatophores.<sup>3,78</sup>

### 3.3. Light-scattering leucophores

Leucophores are a class of light-scattering cells that mainly contribute to bright white patterns observed in cephalopod skin. These cells can be found in many octopuses and cuttles, in the forms of white spots, white stripes, white head bars, and white zebra-like bands (Fig. 5A(i) and (ii)), while their presence in squid is only identified for a few species.<sup>3,29,30</sup> Leucophores are usually situated beneath the aforementioned optically active layers (*i.e.*, chromatophore organs and iridophore cells) and serve as the bottom layer in the general cephalopod skin architecture.<sup>64</sup> Each leucophore is an elongated and flattened cell that contains thousands of membrane-enclosed spherical particles (named leucosomes) near the surface (Fig. 5A(iii)).<sup>3,29,33</sup> These randomly distributed leucosomes

consist of high-refractive-index reflectin proteins and sulfated mucoproteins as the major structural components, and they possess variable sizes with diameters from hundreds of nanometers to a few microns (Fig. 5A(iv)).<sup>33</sup> Note that the size distribution of spherical leucosomes perfectly overlaps with the wavelength range of the visible light. Therefore, leucophores can diffusively reflect incident visible light into all random directions, due to the presence of high-refractive-index disordered structures on the surface, which can be explained and modeled using the Mie scattering mechanism.<sup>33</sup> As a result, leucophores can function like nearly perfect optical diffusers on the background to complement the pigmentary and structural colors produced by the overlying layers made of chromatophores and iridophores. In addition, such broadband-reflecting properties of leucophores span across a wide spectral range from the ultraviolet to the visible and even to the near-infrared (IR) region of the electromagnetic spectrum (*e.g.*, ~70% in reflectance from 300 nm to 1000 nm measured for a *Sepia officinalis* cuttlefish),<sup>80</sup> which allows these cells to reflect light at different wavelengths that match well with incident illuminations,<sup>33</sup> *i.e.*, they appear white under white light, green under green light, or red under red light (Fig. 5B).

For a long time, leucophores were thought to be physiologically static, because no clear evidence of nerve or muscle connections was found in these cells.<sup>3</sup> More recently, it was demonstrated that leucophores found in the dorsal mantle of female *Doryteuthis opalescens* squid are optically active upon the stimuli of a neurotransmitter (ACh) (Fig. 5C).<sup>81</sup> The leucophore-based white stripes in these animals can dynamically switch their appearances from a highly transparent state to a diffusive white-colored state upon activation (Fig. 5C), as quantified by an over 15% increase in the broadband reflectance, and the whole process takes around three minutes.<sup>81</sup>

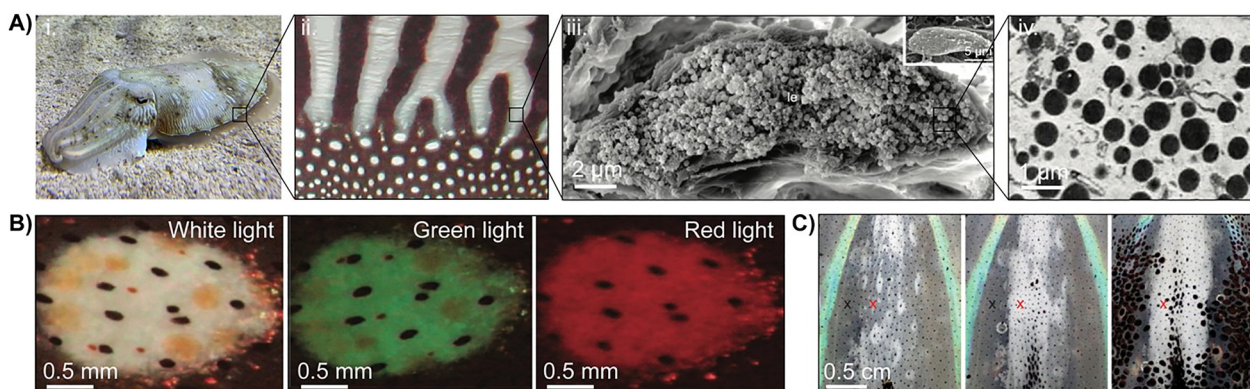


Fig. 5 Light-scattering leucophore cells in cephalopod skin. (A) Leucophore cells at different length scales (from left to right): (i) a digital camera image of a European common cuttlefish (*Sepia officinalis*) on the sandy floor. (ii) a close-up image of the skin of an *S. officinalis* cuttlefish, featuring zebra-like bands with white regions that are mainly composed of leucophores;<sup>33</sup> (iii) a cross-sectional SEM image of a fractured leucophore cell from an *S. officinalis* cuttlefish, featuring densely packed spherical leucosome particles within the cell;<sup>33</sup> (iv) a close-up TEM image of spherical leucosome particles.<sup>33</sup> (B) Optical microscopy images of a single leucophore from an *S. officinalis* cuttlefish displaying different colors when illuminated with lights at different wavelengths.<sup>33</sup> (C) Digital camera images of tunable white stripe in the skin of a female *Doryteuthis opalescens* squid upon the stimuli of a neurotransmitter (ACh), featuring a gradual change in the appearance as indicated by the red cross.<sup>81</sup> The image in Part A (i) was taken by Chengyi Xu and reproduced with permission. The images in Part A (ii)–(iv) and B were reproduced with permission from the IOP Publishing (Copyright©2018). The images in Part C were reproduced with permission from the Company of Biologists Ltd. (Copyright©2013).



This finding represents one of the very few reported examples of tunable leucophores in any cephalopod species, and a comprehensive understanding of possible structural and molecular mechanisms behind such optical modulation remains limited.

## 4. Dynamic optical materials derived from cephalopod skin

The fascinating color-changing and camouflage capabilities of cephalopods are enabled by their synchronically orchestrated bio-optical skin components including chromatophores, iridophores, and leucophores. As such, biological materials that are directly derived from these optically active organs or cells have received much research interest. Two representative types of cephalopod skin-derived materials include (1) reflectin proteins, which are abundant in various light-reflecting photonic structures in cephalopod skin,<sup>82</sup> and (2) xanthommatin-based color pigments, which are predominantly found in pigment granules inside chromatophore organs.<sup>69</sup> These bio-derived materials have exhibited dynamic *in vitro* optical functionalities across multiple length scales and can be rationally engineered or coupled with synthetic materials to achieve unique optical functionalities analogous to (or even exceeding) cephalopod skin.

### 4.1. Reflectin-based optical materials

Reflectin proteins are a family of cephalopod structural proteins that were first discovered in the light-reflecting platelets inside the light organs of Hawaiian bobtail squid (*Euprymna scolopes*) (Fig. 6A(i)–(iv)) and later confirmed present in other optically active skin components such as chromatophores, iridophores, and leucophores.<sup>33,68,77,83</sup> These intrinsically disordered proteins are composed of highly conserved amino acid sequences and contain a large proportion of hydrophilic charged aliphatic and polar aromatic residues (Fig. 6A(v)).<sup>83</sup> Reflectins are known to self-assemble into a variety of responsive photonic structures that underpin cephalopods' dynamic camouflage, for example, multilayered platelets in iridophore cells, spherical leucosome particles in leucophore cells, and aggregates within the sheath cells in chromatophore organs.<sup>33,73,77,84</sup> In addition, reflectins have one of the highest refractive indexes ( $1.591 \pm 0.002$ ) among all reported naturally occurring proteins.<sup>85</sup> While significant progress has been made in understanding their structural and electrical characteristics,<sup>86–92</sup> this review will focus on the exploration of reflectins and their derivatives in dynamic optical applications, as summarized in Table 1.

In a pioneering study, Kramer *et al.* used flow coating to fabricate recombinantly expressed reflectin 1a into uniform thin films (Fig. 6B(i)).<sup>85</sup> The film thickness was adjusted by changing the reflectin 1a solution concentration, which results in different structural colors governed by thin-film interference. A color shift was observed from blue to yellow upon exposure to water vapor, which was caused by an increase in film thickness due to swelling (Fig. 6B(ii)). The unique *in vitro* self-assembling

properties of reflectin were further demonstrated through the formation of iridescent diffraction gratings with tunable micron-scale spacing *via* ionic liquid-facilitated phase separation, featuring defect-free patterns over several millimeters (Fig. 6B(iii)–(v)).<sup>85</sup> Moreover, reflectins were drawn into fibers with tunable diameters using high-viscosity precipitates (Fig. 6B(vi) and (vii)), which exhibited a lack of crystallinity that can minimize unwanted scattering in optical applications.<sup>85</sup> Similarly, both single-layer and multilayer reflectin derivatives (e.g., refCBA from reflectin 1a,<sup>93</sup> 2CX4 from reflectin 1b<sup>94</sup>) were shown to display thickness-dependent structural colors that can be modulated through exposure to water vapor. Besides thin-film interference, wavelength-dependent light scattering was found critical for the dynamic blue color displayed by reflectin films, driven by higher-order self-assembly in the presence of aromatic triggers.<sup>95</sup>

Further efforts have been made to extend the optical functionality of reflectin-based devices from the visible to the IR regions of the electromagnetic spectrum. This was achieved through more substantial modulation of film thickness *via* various external stimuli (e.g., chemical and mechanical) or tunable assembly sizes that red-shift the wavelength of constructive interference into the IR region. Phan *et al.* applied doctor blading to prepare thin films from a histidine-tagged reflectin A1 (RfA1) isoform on a negatively charged graphene oxide-coated silica substrate.<sup>96</sup> Upon exposure to acetic acid vapor, the RfA1 film swelled, increasing its thickness from 207 nm to 394 nm, and thereby shifted its reflection peak from the visible ( $\sim 625$  nm) to the near-IR ( $\sim 1200$  nm) region.<sup>96</sup> Moreover, the same RfA1 was directly coated onto flexible adhesive tape, which could be easily attached onto fabrics for camouflage use.<sup>97</sup> The devices' near-IR reflectance peaks were modulated by mechanically stretching the tape substrate, as the film thickness changed due to the strain-induced Poisson effect.<sup>97</sup> In another study, spherical reflectin B1 nanoparticles were immobilized onto azide-functionalized substrates *via* dibenzocyclooctyne (DBCO)-sulfo-NHS ester-based ligands.<sup>98</sup> These self-assembled nanoparticles exhibited tunable sizes ranging from 170 nm to 310 nm, allowing the reflectance peaks of the resulting films to shift from blue to the near-IR region (Fig. 6C(i)–(iii)).<sup>98</sup>

Electrical stimuli have been explored to trigger color changes in reflectin-based thin-film devices. By leveraging reflectin's exceptional ability to conduct protons, Ordinario *et al.* reported a two-terminal protochromic device that consisted of a RfA1 film sandwiched between a palladium hydride ( $\text{PdH}_x$ ) electrode and a gold (Au) electrode.<sup>99</sup>  $\text{PdH}_x$  served as a proton reservoir, while Au served as an ion-blocking electrode. Upon application of a positive (negative) voltage, protons are injected (withdrawn) from  $\text{PdH}_x$  into (from) the RfA1 layer, resulting in an increase (decrease) in its thickness and thus an  $\sim 20$ -nm red (blue) shift in its peak reflection wavelength (Fig. 6D).<sup>99</sup> In another study, voltage-dependent electrochemical reduction was shown to reversibly change the size of RfA1 assemblies through a charge-neutralization process that closely resembles the phosphorylation-driven condensation observed



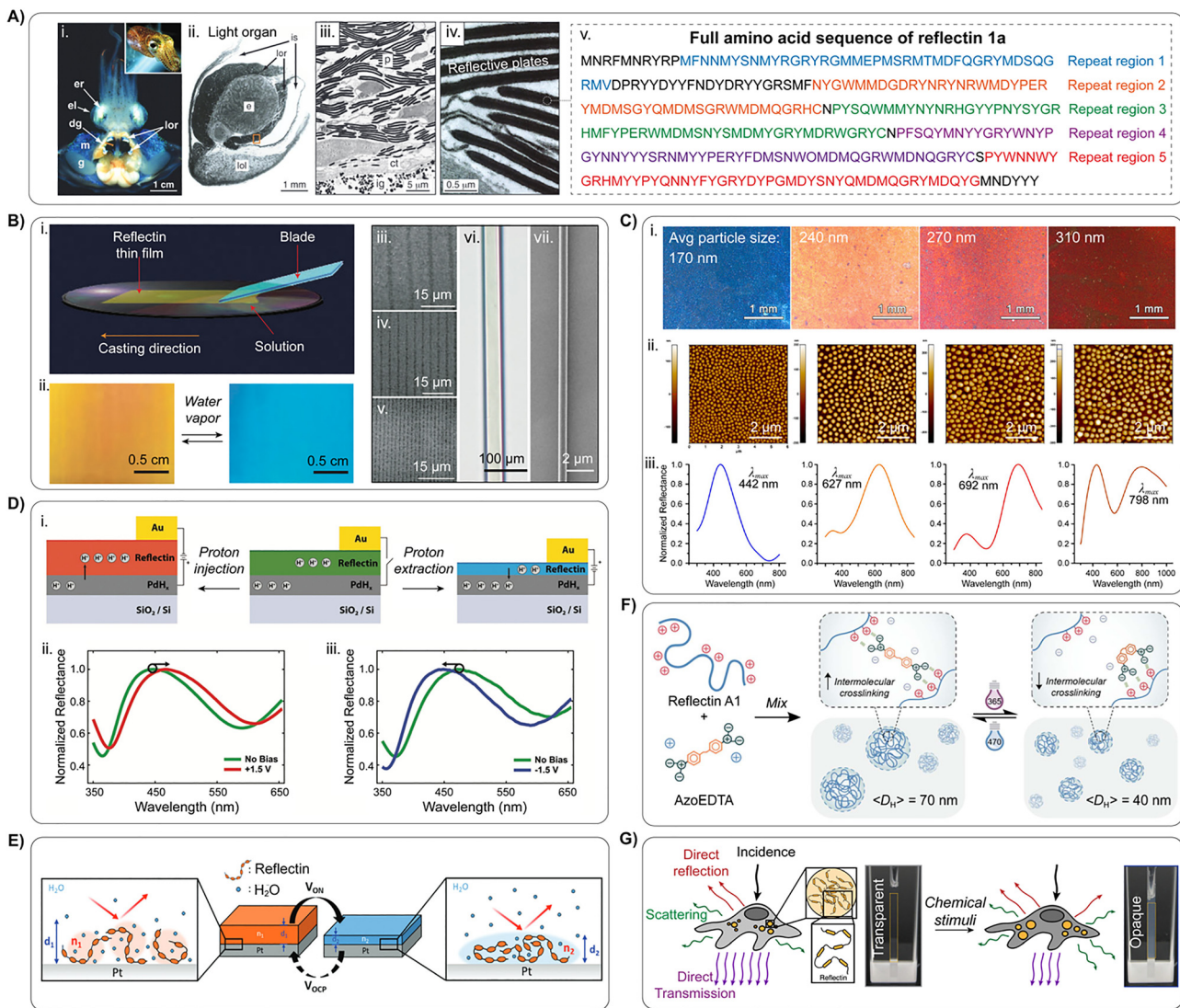


**Fig. 6** Reflectin proteins derived from cephalopod skin as dynamic optical materials. (A) (i) The location of reflective and non-reflective tissues of an *E. scolopes* squid.<sup>83</sup> (ii) A cross-sectional light micrograph of the light organ.<sup>83</sup> (iii) and (iv) Transmission electron microscopy (TEM) images of the orange boxed region in (ii) at different magnifications, showing arrangements of reflective protein platelets.<sup>83</sup> (v) Linear amino acid sequence of a full-length reflectin 1a isoform, showing repeated domains highlighted in different colors.<sup>83</sup> (B) (i) An illustration of the fabrication of a reflectin 1a-based thin film on a rigid substrate by flow coating.<sup>85</sup> (ii) Images of a reflectin 1a-based thin film reversibly changing the color from orange (left) to blue (right) upon the application of water vapor.<sup>85</sup> (iii)–(v) SEM images of diffraction grating made from reflectin 1a, featuring tunable grating spacing; (vi) an optical microscope image of a highly amorphous fiber made from reflectin 1a; (vii) an SEM image of another amorphous fiber made from reflectin 1a with a much smaller diameter.<sup>85</sup> (C) (i) Structural coloration, (ii) atomic force microscope (AFM) images of the surface topography, and (iii) normalized visible-to-near-IR reflectance spectra of monolayers composed of DBCO-conjugated reflectin B1 nanospheres with tunable sizes.<sup>98</sup> The nanospheres were self-assembled and deposited on an azide-functionalized wafer via a Langmuir–Schaefer approach.<sup>98</sup> (D) (i) Schematics of a RfA1-based protochromic device with the application of no bias (middle), a positive bias (left), and a negative bias (right) on the palladium hydride ( $PdH_x$ ) electrode, featuring a thickness change in the constituent RfA1 layer upon proton injection or extraction.<sup>99</sup> (ii) Normalized reflectance spectra for a representative RfA1-based protochromic device before (green curve) and after (red curve) the application of a positive bias of +1.5 V on the  $PdH_x$  electrode.<sup>99</sup> (iii) Normalized reflectance spectra for a representative RfA1-based protochromic device before (green curve) and after (blue curve) the application of a negative bias of -1.5 V on the  $PdH_x$  electrode.<sup>99</sup> (E) Schematics of voltage-induced swelling and shrinkage of a reflectin film on a Pt working electrode, showing simultaneous changes in film thickness and refractive index for structural color modulation.<sup>101</sup> (F) Schematics of photo-controlled electrostatic interactions between RfA1 and a multivalent AzoEDTA-based photoswitch with anionic end groups, showing reversible modulation of assembly size under different light wavelengths.<sup>103</sup> (G) Schematics of a RfA1-expressed human cell before (left) and after (right) applications of chemical stimuli, featuring changes in the size, geometry, and arrangement of the RfA1 nano-agggregates within the cell, which lead to changes in light transmission and reflection. The actual transparency modulation of a cell-containing solution is shown by the optical images.<sup>104</sup> Part A was reproduced with permission from Springer Nature (Copyright © 2004). Part B was reproduced with permission from Springer Nature (Copyright © 2007). Part C was reproduced with permission from the American Chemical Society (Copyright © 2022). Part D was reproduced with permission from John Wiley and Sons (Copyright © 2017). Part E was reproduced with permission from John Wiley and Sons (Copyright © 2025). Part F was reproduced with permission from the Royal Society of Chemistry (Copyright © 2024). Part G was reproduced with permission from Springer Nature (Copyright © 2007).



Table 1 Summary of dynamic optical materials based on cephalopod reflectins. The naming of reflectin proteins follows that used in the original papers

Reflectin-based optical materials	Gene origin	Material production	Device format	Device fabrication	Device substrate	External stimuli	Optical functionality	Ref.
Reflectin 1a	<i>Euprymna scolopes</i>	<i>Escherichia coli</i> ( <i>E. coli</i> ) expression	Thin films	Flow coating	Silicon (Si)	Chemical (water, methanol, ethanol vapors)	Change in reflectance (visible)	85
Reflectin 1a	<i>Euprymna scolopes</i>	<i>E. coli</i> expression	Diffraction gratings	Dipping	Si	—	Interference-based optical gratings	85
Reflectin 1a	<i>Euprymna scolopes</i>	<i>E. coli</i> expression	Fibers	Drawing from precipitates	—	—	Reduced optical scattering	85
Reflectin-based peptide (refCBA) Reflectin 1b and derived peptides (e.g., 2CX4)	<i>Euprymna scolopes</i>	<i>E. coli</i> expression	Thin films (multilayered)	Flow coating & spin-coating	Si	Chemical (water vapor)	Change in reflectance (visible)	93
	<i>Euprymna scolopes</i>	<i>E. coli</i> expression	Thin films	Flow coating	Si	Chemical (water vapor)	Change in reflectance (both specular and scattered components in the visible)	94
Reflectin 2	<i>Sepia officinalis</i>	<i>E. coli</i> expression	Thin films	Spin-coating	Si or glass	Chemical (water vapor)	Change in reflectance and transmittance (visible)	95
Reflectin A1	<i>Doryteuthis pealeii</i>	<i>E. coli</i> expression	Thin films	Doctor-blading	Graphene oxide-coated $\text{SiO}_2/\text{Si}$	Chemical (water, acetic acid vapors)	Change in reflectance (visible to near-IR)	96
Reflectin A1	<i>Doryteuthis pealeii</i>	<i>E. coli</i> expression	Stretchable films	Doctor-blading	Fluorinated ethylene propylene (FEP) tape	Mechanical strain	Change in reflectance (visible to near-IR)	97
Reflectin B1 (ligand conjugated)	<i>Sepioteuthis lessoniana</i>	<i>E. coli</i> expression	Thin films assembled by nanoparticles	Langmuir–Schaefer deposition & drop-casting	Azide-functionalized $\text{SiO}_2$	Chemical (water vapor)	Change in reflectance (visible to near-IR)	98
Reflectin A1	<i>Doryteuthis pealeii</i>	<i>E. coli</i> expression	Thin films	Drop-casting or dip-coating	$\text{SiO}_2/\text{Si}$	Electrical bias	Change in reflectance (visible)	99
Reflectin A1	<i>Doryteuthis opalescens</i>	<i>E. coli</i> expression	Thin films	Drop-casting	Pt/Si	Electrical bias	Change in refractive index (632.8 nm)	101
Reflectin A2 (phytochrome-doped) (azooEDTA-coupled)	<i>Doryteuthis opalescens</i>	<i>E. coli</i> expression	Thin films	Spin-coating	Si	Light	Change in reflectance (visible)	102
Reflectin A1 (azooEDTA-coupled)	<i>Doryteuthis opalescens</i>	<i>E. coli</i> expression	Solution	Solution mixing	—	Light	Change in absorbance (visible) and turbidity	103
Reflectin A1	<i>Doryteuthis pealeii</i>	Human embryonic kidney (HEK) 293 cells	Cells dispersed in solution	Genetic transfection	—	Chemical (ionic strength of NaCl)	Change in transparency (visible)	104

in biological iridophore lamellas.<sup>100,101</sup> This mechanism was experimentally validated on a platinum (Pt) electrode using electrochemical correlative ellipsometry, where applying a small voltage (up to  $-0.8$  V) reduced the RfA1 film thickness and increased its refractive index from 1.36 to 1.40 at a wavelength of 632.8 nm (Fig. 6E).<sup>101</sup> These concurrent changes in film geometry and optical properties show promise for the continued development of iridophore-like, color-changing devices.

Light-responsive reflectin-based devices with tunable optical properties have been developed. One approach is to integrate reflectins with photosensitive molecules, where the light-driven changes are mainly contributed by the photosensitive molecules rather than reflectins. For example, Wolde-Michael *et al.* reported a bilayer device composed of reflectin and phytochrome-1 protein (from *Agrobacterium fabrum*).<sup>102</sup> Due to a photo-induced conformational change in phytochrome between the open and closed states, the phytochrome layer exhibited a color change with its reflectance peak shifting from  $\sim 750$  nm to  $\sim 710$  nm upon exposure to different wavelengths of light, thereby adjusting the overall appearance of the reflectin-phytochrome bilayer device. Another approach is to leverage dynamic inter-/intra-molecular interactions between reflectins and photosensitive molecules upon light exposure. Tobin *et al.* designed a multivalent azobenzene photoswitch (azoEDTA) molecule with anionic end groups to form complex assemblies with RfA1.<sup>103</sup> Photoisomerization of azoEDTA between the *trans* and *cis* states altered its electrostatic cross-linking dynamics with the cationic blocks in RfA1, which enabled repeated modulation of the size and secondary structure of the reflectin-azoEDTA assemblies (Fig. 6F). The average diameter of the assemblies cycled between  $74 \pm 52$  nm and  $39 \pm 25$  nm upon repeated exposure to 365-nm and 470-nm light, resulting in reversible control of solution absorbance and turbidity.

Recently, reflectins have been explored for integration into engineered living cells for stimuli-responsive optical modulation. Chatterjee *et al.* reported the direct expression of a histidine-tagged RfA1 within human embryonic kidney (HEK) 293 cells through transfection with a target vector encoding.<sup>104</sup> Due to the formation of reflectin nano-aggerates, the initially transparent HEK cells became less transparent after transfection, exhibiting an increased level of scattering (*i.e.*, diffuse transmission and reflection). In analogy to the ACh-regulated, transparency-modulating leucophores in *Doryteuthis opalescens*, the RfA1-containing HEK cells were able to modulate their optical transparency in response to chemical stimuli such as sodium chloride (NaCl).<sup>104</sup> An increase in the NaCl concentration from 117 mM to 217 mM resulted in an  $\sim 2$ -fold increase in the solution's diffuse transmittance and reflectance (Fig. 6G). This enhanced scattering was attributed to changes in the size, geometry, and arrangement of reflectin nano-aggerates under varied ionic strength, which significantly altered the visible opacity of the host cells.<sup>104</sup> Similar optical tunability were observed in both transiently and stably transfected RfA1-expressing cells.<sup>105</sup>

## 4.2. Xanthommatin-based optical materials

Naturally occurring pigments are abundant in the pigment granules of cephalopod color-changing chromatophore organs, and they are mainly responsible for the predominant pigmentary coloration exhibited by cephalopod skin. These pigment can be extracted by mixing the cephalopod pigment granules with a hydrochloric acid/methanol solution, followed up by centrifugation and purification, and have been structurally confirmed as ommochromes, including xanthommatin (Xa) and decarboxylated xanthommatin (DC-Xa).<sup>106</sup> Both Xa and DC-Xa are aromatic metabolites of tryptophan formed through biological processes, and their combination enables chromatophores to display a broad range of colors across the visible region of the electromagnetic spectrum.<sup>107</sup> Due to their biocompatibility, optical functionality, and synthetic scalability, Xa-based pigments demonstrate high technological value and have recently been used in various light-related technologies such as cosmetic ingredients,<sup>108–110</sup> paints,<sup>111–114</sup> displays,<sup>115–117</sup> and sensors,<sup>118</sup> as summarized in Table 2.

Pristine Xa is known as a color-changing biochrome depending on its redox states. Kumar *et al.* developed a Xa-based electrochromic device, where Xa was coated onto an indium-doped tin oxide (ITO)-based substrate that was pre-modified with poly(3,4-ethylene dioxythiophene):poly(styrene sulfonate) (PEDOT:PSS) (Fig. 7A(i)).<sup>115</sup> The device was able to switch from yellow under an oxidizing potential ( $+1.5$  V) to red under a reducing potential ( $-1.5$  V), with a red shift in the absorption peak by  $\sim 70$  nm (Fig. 7A(ii) and (iii)).<sup>115</sup> By varying the ratio of Xa and (blue-tinted) PEDOT:PSS, different color combinations were achieved (Fig. 7A(iv)), although they were limited to the yellow-red regions.<sup>115</sup> To improve device scalability, Sullivan *et al.* introduced inkjet printing to prepare Xa-based electrochromic pixels and enabled multilayer printing, array fabrication, and pixel miniaturization with enhanced precision (Fig. 7B(i)).<sup>116</sup> Each pixel could be precisely patterned, with color switchable between yellow and red depending on the redox states of Xa (Fig. 7B(ii)).<sup>116</sup> In addition to electrochemical processes, Xa exhibits a photoreduction-induced color change from yellow to red under solar radiation. Using this mechanism, Wilson *et al.* developed a wearable Xa-based light sensor capable of monitoring light exposure from UV to near-IR *via* chromaticity shifts (Fig. 7C).<sup>118</sup> To enhance the device's light-sensing performance, cystine solution was added to Xa, which enabled radiation-triggered formation of cysteine—a reducing agent that facilitates color change in Xa.<sup>118</sup>

Various inorganic particles (*e.g.*,  $\text{SiO}_2$ ,  $\text{TiO}_2$ ) have been incorporated with the Xa pigment to expand the resulting devices' optical functionality. Using a diatom-inspired biosilification process, Martin *et al.* fabricated Xa-silica nanoparticles (XaNPs) by encapsulating Xa onto silica nanoparticles in the presence of amine-terminated polyamidoamine (PAMAM) dendrimers and monosilicic acid *via* electrostatic interactions (Fig. 7D(i)).<sup>113</sup> A range of neutral colors with varying hues were obtained by adjusting the Xa loading concentration. The resulting XaNPs could be easily processed and casted onto flexible Spandex fabrics, exhibiting homogeneous particle distribution



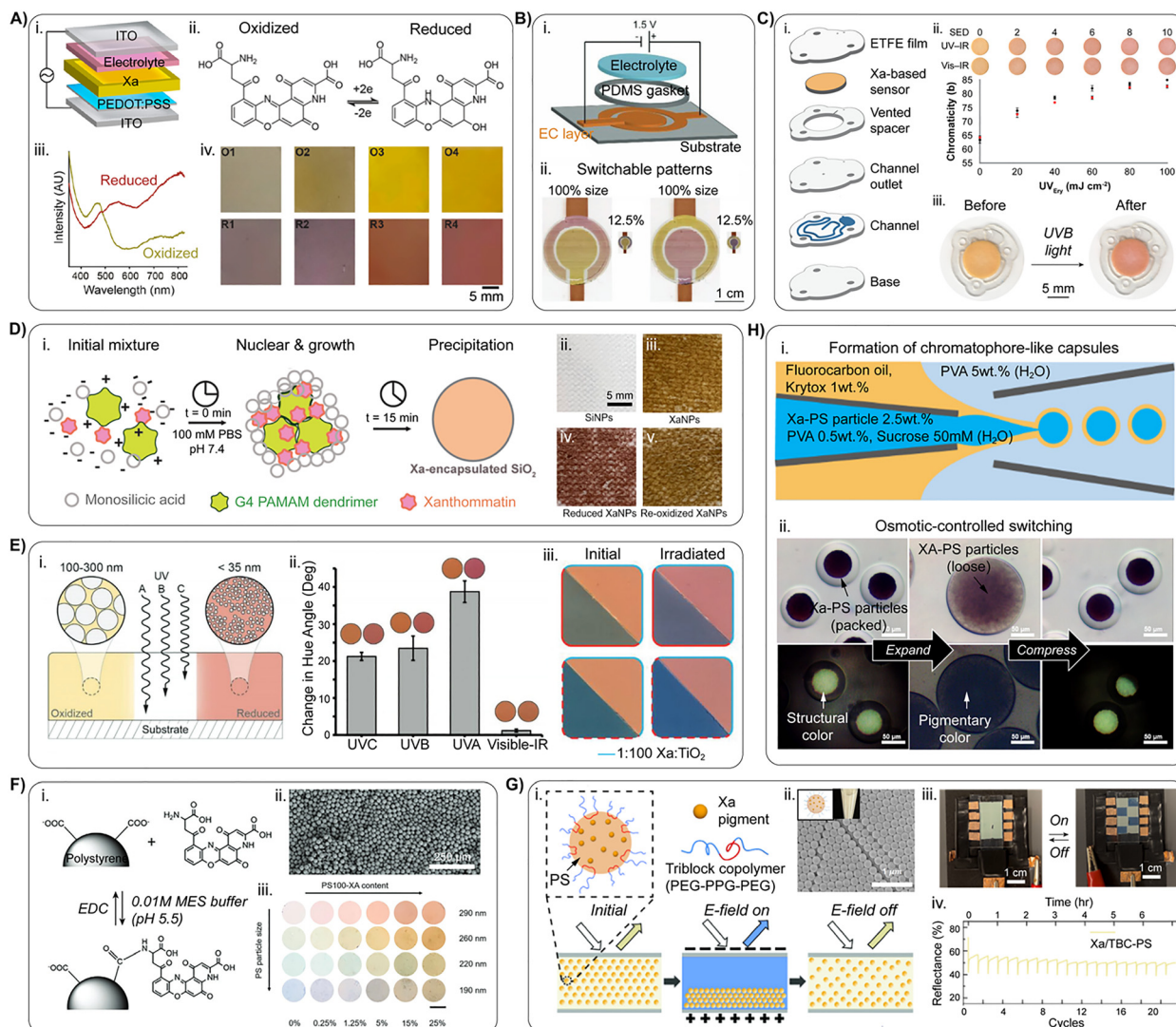


Table 2 Summary of dynamic optical materials based on cephalopod xanthommatin (Xa) pigment

Xa-Based Optical Materials	Material Production Approach	Device Format	Device Fabrication	Device Substrate	External Stimuli	Optical Functionality	Refs
Xa	Chemical synthesis	Thin films	Electrodeposition	PEDOT:PSS-modified ITO	Electrical bias	Change in color (from yellow to red)	115
Xa	Chemical synthesis	Thin films	Inkjet printing Casting	PTF sheet	Electrical bias	Change in color (from yellow to red)	116
Xa	Chemical synthesis (silification)	Nanoparticle coatings	Drop-casting	Chromatography paper	Ultraviolet light	Change in color (from yellow to red)	118
Xa-SiO <sub>2</sub> composite	Chemical synthesis & Composite mixing	Paint films	Spray-coating	Glass & Spandex fabrics	Chemical (ascorbic acid) Ultraviolet light	Change in color (from yellow to red)	113
Xa-TiO <sub>2</sub> composite	Chemical synthesis (carboxylation)	Powder-pressed films	Mechanical press	Polyurethane	Chemical (ascorbic acid) Ultraviolet light	Change in color (from yellow to red)	114
Xa-polystyrene (PS) composite	Chemical synthesis	Colloidal suspension	Suspension	Glass	Nanoparticle size & loading	Change in reflectance (various colors)	111
Xa-PS-Triblock copolymer (TBC) composite	Chemical synthesis	Water-oil-water double emulsion capsules	Capillary-based microfluidic injection	ITO glass	Electrical bias	Change in color (from blue to beige)	117
Xa-PS microcapsules	Chemical synthesis	—	—	—	Chemical (osmotic pressure change due to NaCl concentration)	Color switching between green (structural) and brown (pigmentary)	112

on the individual fibers. Benefiting from XaNPs' mesoporous structures, the color of the XaNP-coated fabrics was tunable by changing the local pH, such as through exposure to ascorbic acid, through a plausible proton-coupled reduction mechanism (Fig. 7D(ii)–(v)).<sup>113</sup> In another study, Martin *et al.* developed a color-changing paint formulation by leveraging the redox-dependent absorption of Xa and the photoelectronic properties of titanium dioxide (TiO<sub>2</sub>).<sup>114</sup> As a common photocatalyst and whitening agent, TiO<sub>2</sub> is known to generate excited electrons from the valence to the conduction band when exposed to light with wavelengths below 400 nm.<sup>119</sup> These excited electrons can readily convert Xa from oxidized (yellow) to reduced (red) states (Fig. 7E(i)). The resulting Xa-TiO<sub>2</sub> exhibited a significant color change under UVA light (wavelength from 315 nm to 400 nm), while negligible change was noticed under visible-NIR light (wavelength above 400 nm) (Fig. 7E(ii)).<sup>114</sup> Furthermore, the devices' color space were expanded into blue-green regions by blending other photo-insensitive natural pigments (*e.g.*, ultramarine) (Fig. 7E(iii)).<sup>114</sup>

Synthetic organic particles have been engineered to produce short-wavelength structural coloration, which can be coupled with the intrinsic long-wavelength pigmentary coloration of Xa pigments to significantly expand the achievable color space. Polystyrene (PS) nanospheres are well-known building blocks for forming photonic crystals with tunable structural colors by adjusting the size and packing of spheres.<sup>120</sup> By tethering Xa onto carboxylic acid-functionalized PS nanospheres, Lin *et al.* fabricated amorphous photonic assemblies with tunable color and contrast by changing the nanosphere size and loading concentration (Fig. 7F(i)).<sup>111</sup> The incorporation of Xa into PS preserved the short-range structural order but disrupted the long-range order in the assemblies, resulting in angle-independent colors (Fig. 7E(ii) and (iii)).<sup>111</sup> In another study, Lee *et al.* functionalized Xa-impregnated PS nanospheres with a triblock copolymer (TBC) made of polyethylene glycol–polypropylene glycol–polyethylene glycol through a swelling–deswelling process (Fig. 7G(i) and (ii)).<sup>117</sup> An electrophoretic display was fabricated by sandwiching the Xa-PS-TBC suspension between two ITO glass electrodes. Upon application of a direct-current (DC) electrical field, negatively charged Xa-PS-TBC particles are attracted to and organized at the positively charged electrode, displaying a blue structural color (Fig. 7E(iii)). Once the electrical field is withdrawn, the particles are redispersed, displaying a light beige color. The incorporation of TBC effectively enhanced the colloidal stability and cyclic reversibility under electrophoretic control (Fig. 7E(iv)).<sup>117</sup> Furthermore, Kim *et al.* fabricated stimuli-responsive double emulsion microcapsules from Xa-functionalized PS particles that can dynamically switch between pigmentary and structural coloration.<sup>112</sup> The microcapsules were produced using a capillary-based microfluidic device to form stabilized water-in-oil-in-water assemblies, with aqueous suspended Xa-PS particles in the core (Fig. 7H(i)).<sup>112</sup> Upon an increase in osmotic pressure (*e.g.*, adding NaCl), the microcapsules underwent shrinkage with densely packed PS particles in the core, revealing bright



**Fig. 7** Xanthommatin (Xa) Pigment Derived from Cephalopod Skin as Dynamic Optical Materials. (A) (i) Schematic of a Xa-based electrochromic device with a multilayered structure.<sup>115</sup> (ii) Proposed chemical structures of Xa in its oxidized (left) and reduced (right) states.<sup>115</sup> (iii) Absorption spectra of oxidized and reduced Xa films on a PEDOT:PSS-modified ITO substrate. (iv) Optical images showing the colors of four independent Xa-based electrochromic devices in oxidized (top) and reduced (bottom) states.<sup>115</sup> (B) (i) Schematic of an inkjet-printed Xa-based electrochromic pixel.<sup>116</sup> (ii) Optical images of miniaturized pixels with similar color-changing performance, showing switchable colors in both outer and inner electrodes depending on the redox state.<sup>116</sup> (C) (i) Schematic of a wearable Xa-based light sensor with patterned microfluidic channels.<sup>118</sup> (ii) Radiation exposure detection by measuring the chromaticity shift in Xa light sensors under varying intensity of erythemally weighted ultraviolet radiation ( $UV_{Er}$ ).<sup>118</sup> (iii) Distinct color change in a cystine-activated Xa light sensor from yellow to red upon exposure to  $1\text{ J cm}^{-2}$  UV light.<sup>118</sup> (D) (i) Synthesis scheme of Xa-encapsulated silica nanoparticles (XaNPs).<sup>113</sup> (ii)–(v) Optical images of a Spandex fabric coated with only silica nanoparticles (SiNPs) or XaNPs at different states (i.e., original, acid-reduced, and re-oxidized).<sup>113</sup> (E) (i) Schematic of photo-induced color change in Xa when incorporated with photo-electronic  $\text{TiO}_2$  nanoparticles of different sizes.<sup>114</sup> (ii) Change in the hue angle of Xa- $\text{TiO}_2$  films upon exposure to various wavelength bands in the UV, visible, and IR regions.<sup>114</sup> (iii) Optical images of Xa- $\text{TiO}_2$  films blended with a photo-insensitive pigment of ultramarine in two different formulations, showing expanded color space and similar photochromic performance.<sup>114</sup> Panel size:  $\sim 500\text{ mm}^2$ . (F) (i) Synthesis of Xa-functionalized PS nanoparticles via surface carboxylic acid groups.<sup>111</sup> (ii) SEM image of amorphous photonic structures formed by mixing both pristine and Xa-functionalized PS nanoparticles.<sup>111</sup> (iii) Optical images showing the achievable color palette by varying the PS nanoparticle size (vertical axis) and the amount of Xa-functionalized PS (horizontal axis) (scale bar: 6 mm).<sup>111</sup> (G) (i) Schematic of an electrophoretic display made from triblock copolymer-stabilized Xa-PS (Xa/TBC-PS) nanospheres. The display color is tunable through reversible particle distribution driven by electrostatic interactions.<sup>117</sup> (ii) SEM image of self-assembled Xa/TBC-PS nanospheres prepared by solution dropcasting on a glass substrate.<sup>117</sup> (iii) An 8-pixel electrophoretic display made from Xa/TBC-PS before (left) and after (right) activation. The electrically activated pixels appeared blue, and the non-activated pixels appeared light beige.<sup>117</sup> (iv) Reflectance intensity at 555 nm for a representative pixel over 22 repeated cycles.<sup>117</sup> (H) (i) Schematic of the fabrication of chromatophore-like capsules using a capillary-based microfluidic device.<sup>112</sup> (ii) Transmission (top) and reflection-mode (bottom) optical microscope images of chromatophore-like capsules reversibly switching between expanded and compressed states upon increased salt concentration, displaying bright green or dark brown colors dictated by pigmentary or structural coloration.<sup>112</sup> Part A was reproduced with permission from the American Chemical Society (Copyright © 2018). Part C was reproduced with permission from the American Chemical Society (Copyright © 2022). Part D was reproduced with permission from the American Chemical Society (Copyright © 2021). Part E was reproduced with permission from John Wiley and Sons (Copyright © 2023). Part F was reproduced with permission from John Wiley and Sons (Copyright © 2021). Part G was reproduced with permission from the American Chemical Society (Copyright © 2025). Part H was reproduced with permission from the Royal Society of Chemistry (Copyright © 2024).

green color from structural coloration (Fig. 7H(ii)). Once the osmotic pressure was removed, the microcapsules slowly returned to an expanded state, and the PS particles became loosely packed with a dominant pigmentary-based brown color.<sup>112</sup>

## 5. Dynamic optical systems inspired by cephalopod skin

Inspired by cephalopod skin, numerous bioinspired materials and technologies have been developed for dynamic light or appearance manipulation. These man-made systems leverage synthetic functional materials and mimic the underlying principles of cephalopod camouflage by learning from (1) the global architecture and function of the skin, and (2) the structure and function of individual bio-optical components (*e.g.*, chromatophores, iridophores, and leucophores) at the cellular or organ level. Through rational material and device engineering, these principles have been successfully translated across the electromagnetic spectrum, from the visible to the IR. In addition to light modulation, shape-morphing strategies – mimicking cephalopod skin papillae–have been explored to dynamically alter surface textures for visual camouflage.

### 5.1. Dynamic optical systems in the visible

At a global scale, the overall architecture and functions of cephalopod skin have inspired the development of advanced bioinspired display and camouflage technologies that function in the visible region. By leveraging technical foundations established for silicon electronics, Yu *et al.* constructed a cephalopod skin-like, flexible monochromatic display with distributed sensing and actuating capabilities (Fig. 8A(i)).<sup>121</sup> Each pixel unit contained a thermochromic leucodye layer that could change color from black to transparent when heated (analogous to chromatophores), a reflective silver layer (analogous to leucophores), a silicon diode layer that could activate the overlying leucodye layer by Joule heating (analogous to muscles attached to chromatophores), a polydimethylsiloxane (PDMS) substrate, and a backside silicon photodetector layer for light sensing (analogous to light-sensitive opsins) (Fig. 8A(ii)).<sup>121</sup> A  $16 \times 16$  array was shown, with each pixel independently addressable (Fig. 8A(iii) and (iv)) and capable of sensing the environment and generate simple patterns to match.<sup>121</sup> By mimicking squid's ability to change body transparency for concealment, Kim *et al.* developed a camouflage display for aquatic environments (Fig. 8B(i)).<sup>122</sup> The PDMS-encapsulated display consisted of (1) six distributed tungsten trioxide ( $WO_3$ )-based electrochromic pixels for color change between transparent and deep blue *via* redox reactions and (2) a wireless control system that allows remote manipulation of individual pixels *via* Bluetooth and near-field communication (Fig. 8B(i)).<sup>122</sup> This integrated system was able to dynamically blend into a gradually dimmed aquatic environment (Fig. 8B(ii)), although its long-term stability is currently limited due to water permeation.<sup>122</sup> Similar environmentally responsive

electrochromic displays were reported to emulate cephalopods' neurological process by displaying different colors based on the external sound level.<sup>123</sup>

Moving down to the organ/cellular scale, the structures and working principles of individual cephalopod skin components (*e.g.*, chromatophores and iridophores) have attracted extensive attention for bioinspired adaptive optical systems that control visible light. Zhou *et al.* introduced a color-changing skin by mimicking the intricate interplay between chromatophores and iridophores (Fig. 8C(i)).<sup>124</sup> To mimic chromatophores, a temperature-responsive poly(*N*-isopropyl acrylamide) (PNIPAAm)-based hydrogel film was fabricated by dispersing pigments including natural cuttlefish ink (brown),  $FeCl_3$  solution (yellow), and Ponceau S (pink) to render different pigmentary colors. The hydrogel film could shrink upon heating above its volume-phase transition temperature and thus reversibly change its size and color concentration when exposed to an IR laser. To mimic iridophores, structurally colored layers exhibiting green and blue hues were fabricated using PS nanoparticles. By overlaying the artificial chromatophore and iridophore layers, multiple color combinations were obtained and could dynamically respond to environmental thermal stimuli (Fig. 8C(ii) and (iii)).<sup>124</sup> In another study, Han *et al.* reported a light-responsive artificial chromatophore (LAC) capable of appearance modulation *via* light-driven actuation.<sup>125</sup> A single LAC consisted of two active components: a photoactive muscle and a stretchable, color-changing sac (Fig. 8D(i)). The photoactive muscle was made of a PNIPAAm hydrogel embedded with photothermal polydopamine (PDA) nanoparticles, which generated heat upon light exposure, causing the hydrogel matrix to shrink. The elastic sac was made of an acrylic acid hydrogel with ionic crosslinking ( $Fe^{3+}$ ) that could be stretched over 200%. Through multi-material projection micro-stereolithography, these two components were printed to form an LAC unit that could reversibly change its visual appearance (*i.e.*, black-to-white ratio) in response to both temperature and light stimuli (Fig. 8D(ii) and (iii)).<sup>125</sup>

Besides tunable optical properties, cephalopod skin has also inspired numerous luminescence-based technologies involving the control of light emission in response to external stimuli such as light, electricity, heat, strain, and chemical reactions.<sup>126–130</sup> Morin *et al.* developed pneumatically actuated soft camouflage crawling robots by embedding a network of microfluidic channels into a deformable silicone rubber (Fig. 9A(i)).<sup>126</sup> Injection of different liquids into the microfluidic channels allowed dynamic modulation of the pigmentary, fluorescent, and chemiluminescent appearances of the soft robots (Fig. 9A(ii) and (iv)).<sup>126</sup> In addition, Wang *et al.* developed a chromatophore-like, electro-mechano-chemical responsive system using a spiropyran-blended mechanochromic elastomer for active fluorescent modulation (Fig. 9B).<sup>127</sup> Upon mechanical stretching, the elastomer switched from light yellow to blue, accompanied by an increase in fluorescence emission intensity due to a ring-opening reaction of spiropyran to form merocyanine. By sandwiching the mechanochromic elastomer between two transparent electrodes, crater-like patterns were formed under high voltage due to



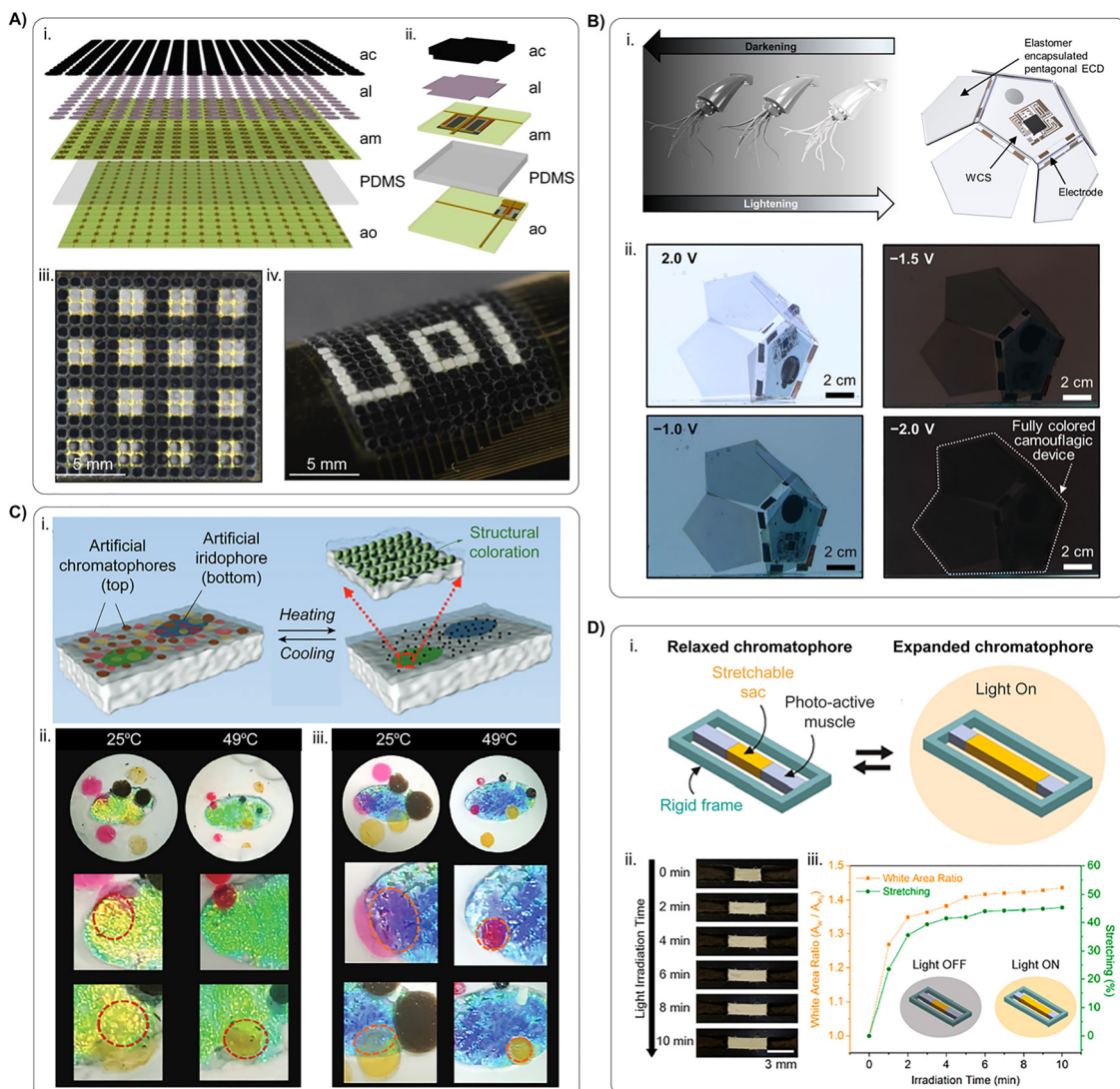


**Fig. 8** Cephalopod skin-inspired systems with tunable optical properties in the visible. (A) (i) Illustration of a cephalopod skin-like, multiplexed flexible monochromatic display with distributed sensing and actuating capabilities.<sup>121</sup> (ii) Each individual unit within the array features a five-layer device structure consisting of an artificial chromatophore (ac), an artificial leucophore (al), artificial muscle (am), a PDMS substrate, and an artificial opsin unit (ao). Optical images of a multiplexed display with 256 active pixel units, displaying (iii) spatial patterns (e.g., dots) and (iv) letters of 'U o l' even when bent.<sup>121</sup> (B) (i) Squid skin-inspired camouflage display for aquatic environments, featuring tunable body transparency in response to environmental lighting.<sup>122</sup> The display consists of an array of six electrochromic display pixels integrated with a wireless control system. (ii) Demonstration of the operation of the wireless adaptive camouflage display in response to gradually dimming underwater lighting conditions through a voltage-controlled electrochromic process.<sup>122</sup> (C) (i) Schematics of a cephalopod color-changing skin that mimics the interplay between size-changing pigmentary chromatophores and structurally colored iridophores.<sup>124</sup> (ii) and (iii) Various colors produced by overlaying green or blue iridophores with thermally responsive chromatophores that undergo volume shrinkage at elevated temperatures.<sup>124</sup> (D) Schematics of the working mechanism of a light-responsive artificial chromatophore (LAC), featuring dynamic actuation of a stretchable sac and photo-active muscles under light.<sup>125</sup> (ii) Light-induced actuation of a LAC unit over time, showing expansion in the white area (i.e., stretchable sac).<sup>125</sup> (iii) Quantitative characterization of the light-induced strain and white area ratio in a representative LAC as a function of light irradiation time.<sup>125</sup> Part A was reproduced with permission from the National Academy of Sciences (Copyright © 2014). Part B was reproduced with permission from Springer Nature (Copyright © 2024). Part C was reproduced with permission from John Wiley and Sons (Copyright © 2025). Part D was reproduced with permission from the American Chemical Society (Copyright © 2021).

electrostatic attraction-induced wrinkling instability, thereby revealing bright red fluorescent patterns at the strained crater edges, with intensity tunable by adjusting the electric field strength.<sup>127</sup> Inspired by the regenerative ability of cephalopod skin, self-healing functionality was further incorporated into mechanoluminescent skins *via* dynamic supramolecular interactions involving boroxine and hydrogen bonds.<sup>128</sup>

The mechanoluminescence performance was able to fully recover even after severe mechanical damage.<sup>128</sup> In another study, Larson *et al.* developed a cephalopod-inspired electroluminescent skin, featuring a five-layer architecture composed of a zinc sulfide (ZnS) phosphor-based light-emitting layer sandwiched between two ionic hydrogel electrodes and encapsulated by a pair of silicone shells (Fig. 9C(i)).<sup>129</sup>

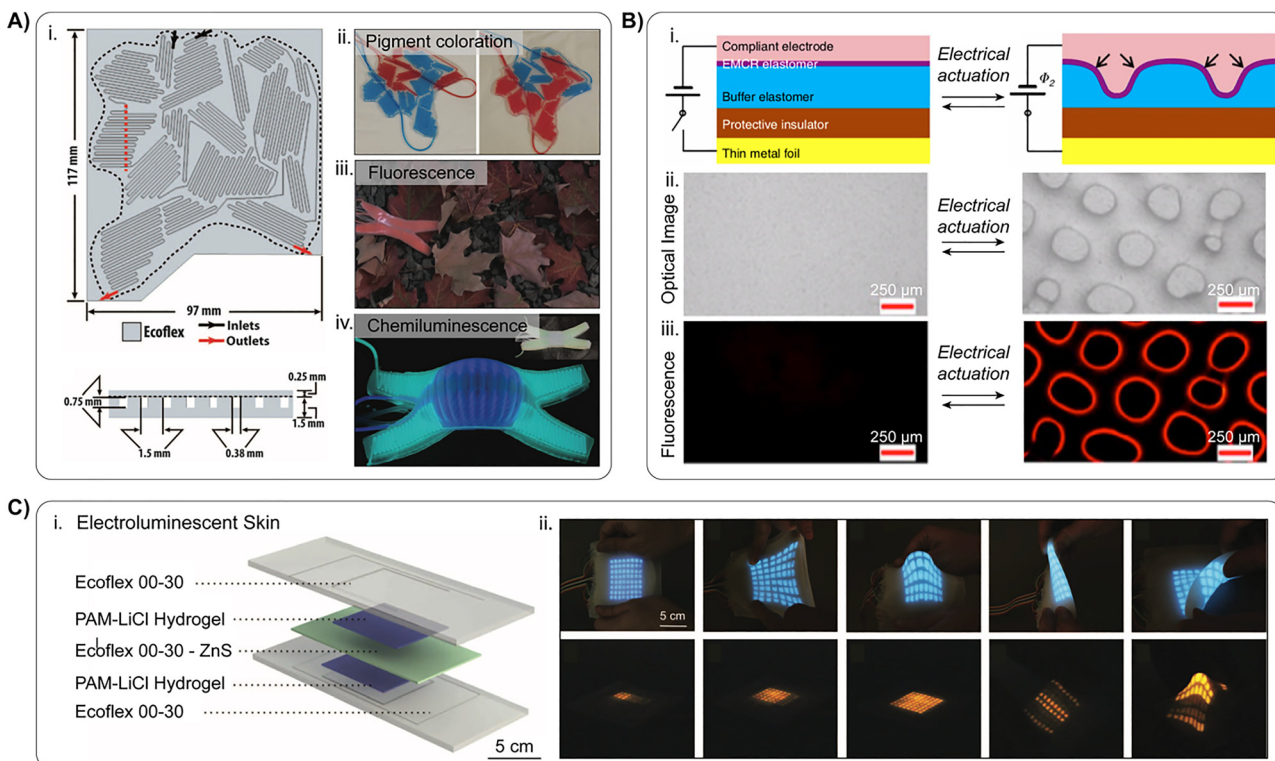


**Fig. 9** Cephalopod skin-inspired systems with light-emitting functions in the visible. (A) (i) Top view (top) and cross-sectional view (bottom) of the body design of a cephalopod-inspired soft camouflage crawling robot, featuring microfluidic channels embedded in a silicone matrix.<sup>126</sup> Optical images of the cephalopod-inspired soft robot showing various camouflage displays, including (ii) pigmentary, (iii) fluorescent, and (iv) chemiluminescent patterns.<sup>126</sup> (B) (i) Cross-sectional schematics of a chromatophore-like, electro-mechano-chemical responsive (EMCR) device before (left) and after (right) electrical actuation, featuring an electrically induced deformation of the EMCR elastomer. (ii) Optical microscopy images of an EMCR device before (left) and after (right) electrical actuation, featuring dynamic surface structures. (iii) Fluorescent microscope images of the same EMCR device before (left) and after (right) electrical actuation, featuring dynamic fluorescent patterning.<sup>127</sup> (C) (i) Schematic of a cephalopod-inspired electroluminescent skin with a five-layer device structure.<sup>129</sup> (ii) (Top) Digital camera images of a multiplexed electroluminescent skin (with blue-light emission) under various deformation modes, including stretching, rolling, folding, and wrapping. (Bottom) Digital camera images of another electroluminescent skin (with orange-light emission) displaying various patterns.<sup>129</sup> Part A was reproduced with permission from The American Association for the Advancement of Science (Copyright©2012). Part B was reproduced with permission from Springer Nature (Copyright©2014). Part C was reproduced with permission from The American Association for the Advancement of Science (Copyright©2016).

The electroluminescent layer could emit light in different colors depending on the type of metal dopant in the ZnS. Multipixel soft skins were shown to maintain consistent light-emitting performance under various deformation modes, including stretching, rolling, folding, and wrapping (Fig. 9C(ii)).<sup>129</sup>

## 5.2. Dynamic optical systems in the infrared (IR)

By translating the underlying working principles of cephalopod chromatophores and iridophores from the visible to the IR region, Xu *et al.* developed an adaptive IR-reflecting camouflage system that allows on-demand manipulation of the reflection of IR radiation across the short-wavelength to long-wavelength IR regions (Fig. 10A).<sup>131</sup> The system featured an optically active area consisting of a dielectric elastomer-based substrate overlaid with reconfigurable IR-reflecting photonic coatings.<sup>131</sup> The dielectric elastomer could be mechanically or electrically actuated to change size and shape (analogous to chromatophores), which in turn changes the surface microstructures (analogous to iridophores) between highly wrinkled and flat states, thereby enabling drastic modulation of the specular and diffuse

components of the surface IR reflection (Fig. 10A(i)–(iii)). Broadband IR reflection modulation across a wide IR range (with wavelengths between 1.5  $\mu$ m and 15  $\mu$ m) was achieved using a reconfigurable 20-nm-thin IR-reflective aluminum coating (Fig. 10A(iv)), while narrowband modulation at specific IR wavelengths (e.g., 3, 4, and 5  $\mu$ m) was realized by constructing Bragg reflectors made of alternating TiO<sub>2</sub> and SiO<sub>2</sub> layers, with thicknesses designed based on the quarter-wavelength principle for maximized peak reflectance.<sup>131</sup> When integrated with a temperature sensor, the system was able to detect small temperature variations in the environment and autonomously adjust IR-reflecting properties and corresponding thermal signatures. As a proof-of-concept, active IR camouflage was demonstrated by reversibly hiding and revealing arbitrary patterns (e.g., a squid shape) into the thermal background with a sub-second response time under an off-the-shelf IR camera.<sup>131</sup>

In several follow-up studies, various IR-reflecting photonic components have been developed for integration onto or into similar stretchable elastomer-based platforms, with their surface morphologies and IR properties tunable upon mechanical

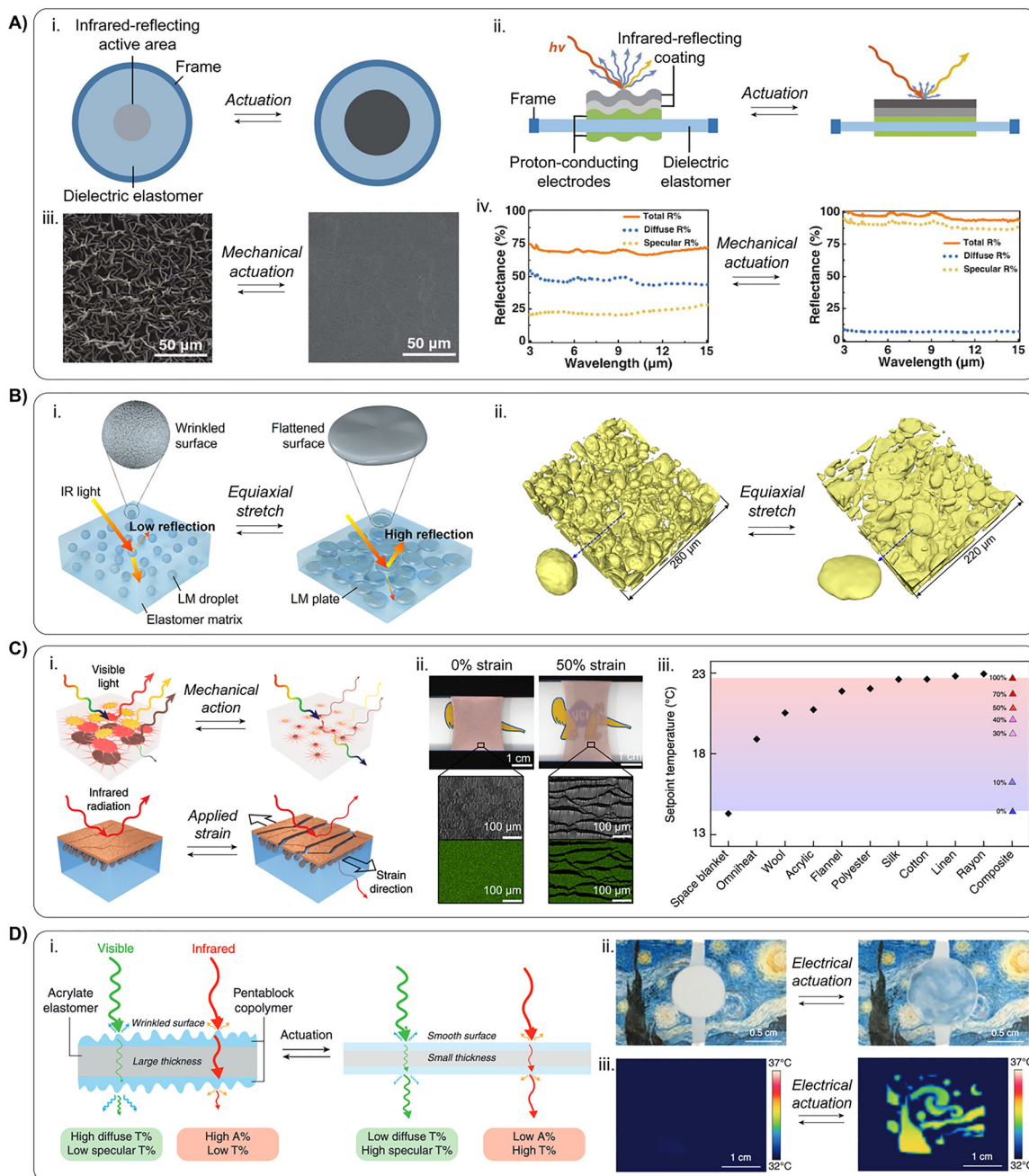


**Fig. 10** Cephalopod skin-inspired dynamic optical systems in the infrared (IR). (A) (i) Top-view schematics of a dielectric elastomer-based adaptive IR-reflecting camouflage system with a size-variable IR-reflecting active area upon actuation, resembling chromatophores.<sup>131</sup> (ii) Cross-sectional schematics of the same IR-reflecting camouflage system, showing iridophore-inspired tunable surface morphology of the IR-reflecting coatings upon actuation.<sup>131</sup> (iii) SEM images of the morphology of a 20 nm aluminum (Al)-coated IR-reflecting system before (left) and after (right) mechanical actuation, featuring a drastic transition from highly wrinkled to flat, smooth surfaces.<sup>131</sup> (iv) Broadband IR reflectance modulation of the Al-coated IR-reflecting system before (left) and after (right) mechanical actuation, showing strain-tunable total, diffuse, and specular reflectance.<sup>131</sup> (B) (i) Side-view schematics of a chromatophore-inspired, liquid metal-dispersed elastomer with variable size and surface morphology under equiaxial stretch.<sup>133</sup> (ii) 3D-reconstructed micro-CT images of the composite with 30 vol% of liquid metal doping under 0% (left) and 200% (right) equiaxial strain.<sup>133</sup> (C) (i) Schematics of a chromatophore-inspired dynamic thermoregulatory composite featuring tunable IR transparency via microcrack engineering.<sup>134</sup> (ii) Optical images of a representative composite before (left) and after (right) the application of 50% uniaxial strain. Insets: SEM morphology images (top) and elemental maps (bottom) at 0% and 50% strain.<sup>134</sup> (iii) Plot of estimated environmental setpoint temperatures at which an individual would remain comfortable. Quantitative comparisons were made between the cephalopod-inspired composite and other commonly available fabric materials, showing a large tunable thermo-comfort window of the composite upon strain.<sup>134</sup> (D) (i) Cross-sectional schematics of a *Japetella heathi* squid-inspired system for dynamic multispectral transparency modulation across the visible and IR regions, showing active control of the total, diffuse, and specular transmittance through actuation-induced geometrical and morphological changes.<sup>136</sup> (ii) Optical images of a multispectral transparency-modulating device functioning in the visible region upon electromechanical actuation.<sup>136</sup> (iii) IR camera images of the same multispectral transparency-modulating device functioning in the thermal IR region upon electromechanical actuation by reversibly revealing and hiding the modified *Starry Night*.<sup>136</sup> Part A was reproduced with permission from The American Association for the Advancement of Science (Copyright © 2018). Part B was reproduced with permission from Elsevier Ltd. (Copyright © 2023). Part C was reproduced with permission from Springer Nature (Copyright © 2019). Part D was reproduced with permission from John Wiley and Sons (Copyright © 2020).



or electromechanical stimuli. As an example, Liu *et al.*, embedded copper (Cu) nanostructures into a thermoplastic elastomer made of styrene–ethylene–butylene–styrene (SEBS).<sup>132</sup> The presence of mechanical mismatch between the Cu and the soft SEBS matrix led to the formation of distinct nano- or micro-structures on the SEBS surface upon applied tensile or compressive strains, which in turn resulted in different thermal appearances for dynamic IR signature management.<sup>132</sup> Similarly, liquid metal (LM) microdroplets were dispersed into silicone elastomers.<sup>133</sup> Upon equiaxial strain, the LM microdroplets underwent shape transformation due to their malleable form factor, transitioning from

contracted dots with wrinkled surfaces to expanded plate-like discs with flat surfaces, thereby enabling dynamic modulation of IR reflection and emissivity (Fig. 10B).<sup>133</sup>

Besides reflection, other IR radiative properties (*e.g.*, transmission, absorption, and emissivity) have been explored using cephalopod-inspired designs. By mimicking the opening and closure of chromatophores, Leung *et al.* developed a dynamic IR composite with tunable IR transparency through microcrack engineering (Fig. 10C(i)).<sup>134</sup> In their design, a nanostructured Cu film was deposited through glancing angle deposition, with extended Cu pillars anchored into a SEBS elastomer. Upon uniaxial

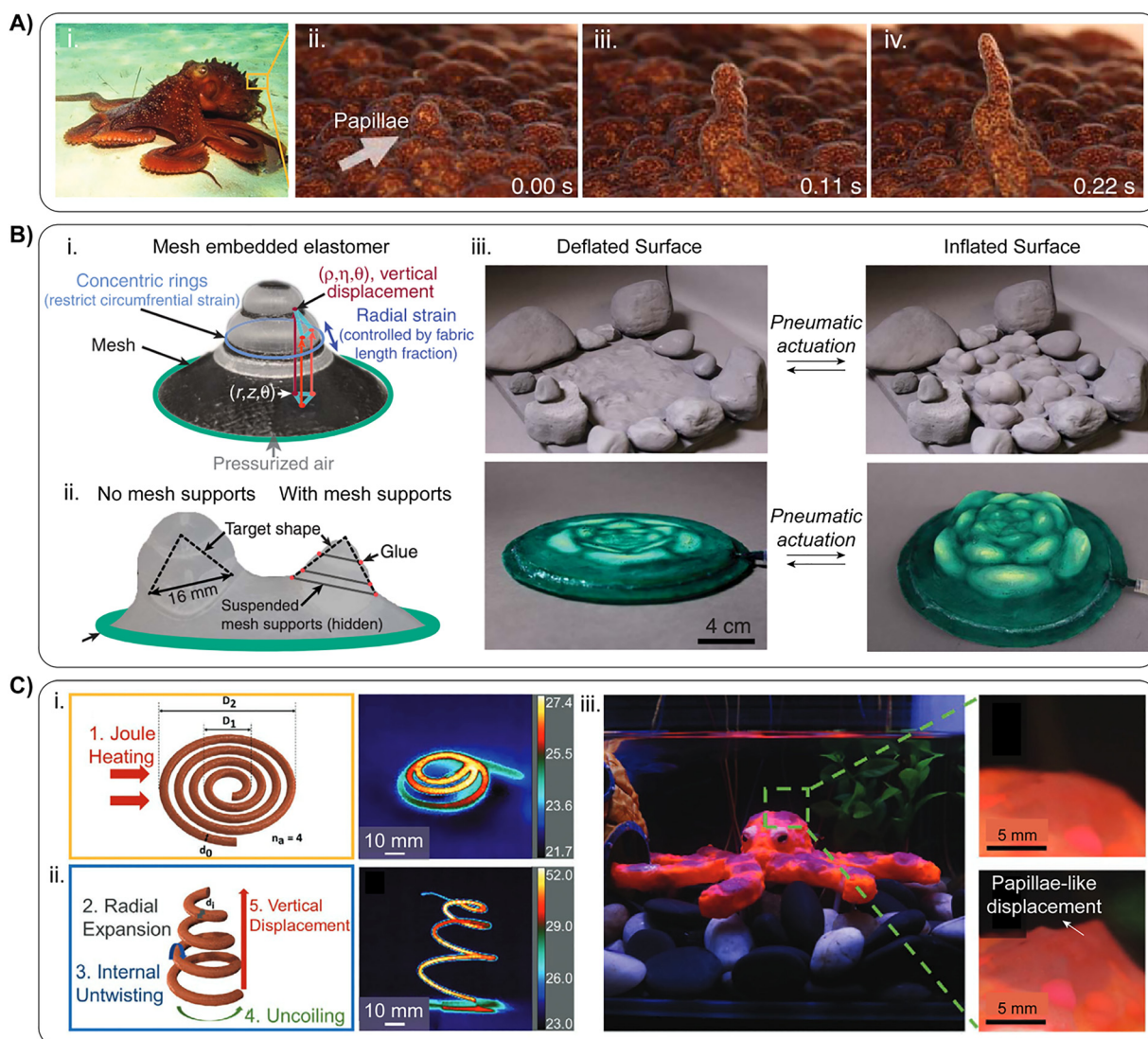


**Fig. 11** Cephalopod skin-inspired visual shape-morphing systems. (A) (i) A *Macroctopus maorum* octopus sitting on the ocean floor, showing actuated papillae in the skin.<sup>138,139</sup> (ii)–(iv) One of the octopus's skin papillae was rapidly actuated and displaced within 0.22 s. (B) (i) Schematic of a pneumatically actuated artificial papilla made from a circumferentially constrained and radially stretched elastomer.<sup>138</sup> (ii) Incorporation of suspended mesh supports enables high-fidelity deformation.<sup>138</sup> (iii) Demonstrations of the shape-morphing capability of the papillae-inspired surfaces, mimicking rocks (top) and a *Graptoveria amethorum* succulent plant (bottom).<sup>138</sup> (C) (i) Schematic (left) and temperature map (right) of a papillae-inspired, spirally twisted, thermally responsive fiber coil before Joule heating, feature a flat profile.<sup>139</sup> (ii) Schematic (left) and temperature map (right) of the same fiber coil after Joule heating, exhibiting clear vertical extension due to thermally induced uncoiling.<sup>139</sup> (iii) Integration of an actutable fiber coil in an octopus replica.<sup>139</sup> Insets: Papillae-like skin displacement are shown upon heating. Part A was reproduced with permission from The American Association for the Advancement of Science (Copyright © 2017) and John Wiley and Sons (Copyright © 2021). Part B was reproduced with permission from The American Association for the Advancement of Science (Copyright © 2017). Part C was reproduced with permission from John Wiley and Sons (Copyright © 2021).



strain, microcracks were formed in the elastomer-bound Cu due to mechanical mismatch, allowing more IR radiation to transmit through the microcracks (Fig. 10C(ii)). By increasing the applied strain from 0% to 50%, the average total IR transmittance increased from ~1% to ~24%, corresponding to an increase in the transmitted heat flux from ~248 W m<sup>-2</sup> to ~307 W m<sup>-2</sup>. This substantial change in radiative heat transfer readily enabled the use of this composite in a wearable thermoregulatory sleeve, theoretically allowing the wearer to maintain thermal comfort across an environmental setpoint temperature window of ~8.2 °C (Fig. 10C(iii))).<sup>134</sup> Later, Badshah *et al.* demonstrated scalable manufacturing of similar composites with a low estimated material cost of ~0.1 US\$ per m<sup>2</sup>, with comparable dynamic heat-regulating performance validated in beverage packaging scenarios.<sup>135</sup> In another work, Xu *et al.* draw inspiration from the *Japetella heathi* squid and designed a single device to achieve unprecedented dynamic modulation of multispectral light transmission across the visible and far-wavelength IR regions (wavelengths between 400 nm and 16.6 μm) (Fig. 10D(i))).<sup>136</sup> A tri-layer device architecture was constructed with a pair of IR-transparent block copolymers (PBCs) sandwiching an IR-absorbing acrylate elastomer. Upon mechanical actuation, the device's broadband specular-to-diffuse transmission ratios were modulated by >3000-fold in the visible, due to the strain-dependent reorganization of surface microstructures in the IR-transparent PBCs, and by >4-fold in the IR, due to the strain-dependent thickness in the IR-absorbing acrylate elastomer. This exceptional IR transparency-modulating performance was maintained under electromechanical actuation, featuring a rapid response time of ~570 ms and excellent cycling stability of over 2000 cycles for unprecedented multispectral camouflage (Fig. 10D(ii) and (iii))).<sup>136</sup> This device platform was further modified by incorporating a stimuli-responsive acene-based dye that allowed tuning of its absorption peak and enabled dynamic near-IR appearance modulation.<sup>137</sup>

### 5.3. Visual shape-morphing systems

Various approaches have been employed to mimic the visual shape-morphing cephalopod papillae by converting 2D planar surfaces into complex 3D shapes (Fig. 11A). As an example, Pikul *et al.* introduced a circumferentially constrained and radially stretched elastomer, featuring a flexible but inextensible fiber mesh patterned and embedded in a silicone elastomer (Fig. 11B(i))).<sup>138</sup> During pneumatic actuation, the fiber mesh provided mechanical constraints that could guide preferential deformation of the soft elastomer into pre-designed shapes. By designing different mesh patterns, 3D surfaces with positive, negative, and zero Gaussian curvatures were achieved and could be combined to form complex asymmetric 3D shapes with hierarchical features upon inflation at frequencies of up to 1 Hz.<sup>138</sup> To further improve the fidelity of high-aspect-ratio deformations, suspended mesh supports were incorporated beneath the elastomer to limit circumferential expansion (Fig. 11B(ii))). Using this mechanism, reconfigurable camouflage surfaces were fabricated and programmed to shapeshift from 2D patterns into complex, large-area shapes resembling

stones and plants (Fig. 11B(iii))).<sup>138</sup> In another work, Fei *et al.* designed a papillae-inspired malleable skin by embedding spirally twisted, thermally responsive fiber coils (made of Cu wire-wrapped nylon fibers) in a silicone elastomer (Fig. 11C(i))).<sup>139</sup> By printing a stretchable liquid metal-based electrode network, Joule heating was applied to the Cu wire with a maximum temperature up to 52 °C. This temperature increase triggered the spontaneous uncoiling of the spirally twisted nylon fibers, resulting in out-of-plane vertical displacement (Fig. 11C(ii))). A small voltage of 0.02 V mm<sup>-1</sup> was sufficient to generate up to 2000% strain, which readily enabled visible skin texture modulation in a cephalopod replica (Fig. 11C(iii))).<sup>139</sup>

## 6. Summary and perspectives

In summary, cephalopods, as a class of marine invertebrates, are known for their fascinating color-changing and camouflage abilities. These soft-bodied animals showcase a vast repertoire of camouflage tactics by dynamically modulating the color, pattern, transparency, contrast, bioluminescence, texture, and even behavior. These dazzling visual feats are physically enabled by sophisticated skin architectures at cellular levels that are generally composed of optically active organs and cells including pigment-rich chromatophores, reflective iridophores, and diffusive leucophores. The synergistic function of thousands (or even millions) of these tiny bio-optical components allows cephalopod skin to dynamically interact with light, functioning like bioelectronic displays. As such, cephalopods and their adaptive skin have garnered much research attention for the development of dynamic optical materials and systems. For example, biological materials, such as reflectin proteins and Xa pigments, have been derived from cephalopod skin and readily enabled various *in vitro* color-changing and camouflage devices. Besides, artificial materials and systems that featured unprecedented optical functionalities have also been developed by drawing inspiration from the underlying principles of natural malleable cephalopod skin. Altogether, this review article presents a long-overdue comprehensive overview of cephalopod camouflage and recent advances in cephalopod-derived and -inspired optical materials and technologies, with the goal of stimulating interdisciplinary research across cephalopod biology, materials science, and engineering domains.

Moving forward, vast challenges and opportunities exist to further our understanding of the biological materials (e.g., reflectins) behind cephalopod's camouflage feats and development of bioinspired optical materials and technologies. Despite the important role of reflectins in cephalopods' optical functionalities, important knowledge gaps remain regarding the molecular structure–function relationships of these intrinsically disordered proteins, as well as their self-assembly into various forms under physiological conditions. The conformational changes within reflectins upon different environmental stimuli (e.g., ionic concentration, pH) are not well understood at the molecular level. In addition, although reflectins have



been studied in a few isoforms from select cephalopod species, the specific sequence motifs responsible for their hierarchical assembly remain underexplored, with limited information linking molecular features to macroscopic optical functionality. This knowledge gap is further complicated by the diversity of wild-type isoforms across cephalopod species. Although not discussed in the scope of this review, reflectins are among the best naturally occurring protein-based proton conductors;<sup>21,91,92</sup> however, it remains unclear whether this remarkable bioelectrical property contributes to rapid optical switching *via* signal transduction, particularly given our limited understanding of reflectin-membrane interactions in color-changing cells. While substantial interdisciplinary effort is needed to address these gaps, elucidating these mechanisms would inform a multiscale approach to effectively utilize or engineer reflectin-based biomolecules and guide the rational design of synthetic or bio-hybrid materials with cephalopod-like functionalities, for example, building LEGO-like block copolymers with building blocks inspired by reflectins' functional motifs.

Although the cellular-level understanding of the bio-optical components within cephalopod skin is largely established, no existing artificial device has yet been developed that fully replicates these dynamic structures with comparable sophistication, performance, and efficiency. In essence, nature evolves based on a "just-enough" principle by balancing functionality with limited available materials, where often non-ideal structures are grown *via* a bottom-up approach. While traditional silicon-based electronics and emerging soft electronics offer ultrahigh manufacturing precision (not to mention access to a vast library of exotic materials), existing cephalopod-inspired optical devices are still fabricated *via* a top-down approach and remain largely in the proof-of-concept stage. One promising route forward is the bottom-up growth of hybridized living optics, where biological components (*e.g.*, cells, organs) are utilized to produce dynamic optical materials and structures.<sup>140</sup> To achieve this, inspiration can be drawn from recent success in organic electronics, such as genetically targeted chemical assembly, in which organic semiconductors are synthesized *in situ* to form self-assembled structures directly at cellular interfaces.<sup>141</sup>

In addition, nearly all prior work has attempted to mimic only single (or very few) aspects of cephalopod skin under restricted operating conditions. An emerging direction is to design standalone soft machines that integrate multiple optical and mechanical modalities, such as color change, texture modulation, luminescence, and locomotion, to better emulate natural camouflage. While cephalopod-inspired multimodal camouflage has been shown in some exploratory devices, their pattern resolution is often limited with relatively low spatio-temporal fidelity, in comparison to the (at least) thousands of color-changing cells and/or organs found in living cephalopod skin. Moreover, the scalability of these man-made systems is still low due to the requirement of exotic materials and often complex manufacturing processes. Additional consideration should be given to enhancing device reliability and robustness under extreme or varying environments (*e.g.*, temperature,

humidity, background lighting), which remain largely underexplored. Furthermore, we note that the same principles underpinning cephalopods' dynamic color-changing behavior can be further extended to engineer stimuli-responsive systems with spectral responsiveness beyond the already-demonstrated visible and IR regions, into other technologically valuable domains such as the ultraviolet and terahertz. This can be potentially achieved through the incorporation of novel materials and photonic structures (*e.g.*, metasurfaces).

So far, very few works have demonstrated cephalopod-like distributed neural control mechanisms enabled by their highly sophisticated peripheral nervous systems (given that nearly two-thirds of cephalopod neurons are distributed across their skin). Indeed, open-loop control with limited feedback has been implemented in most reported cephalopod-inspired optical systems. Moving forward, improved real-time environmental awareness can be achieved by constructing closed-loop control systems through the integration of multimodal, distributed sensory networks capable of detecting various signals (*e.g.*, light, temperature, force, chemicals). Meanwhile, it is important to maintain low power consumption in these artificial systems, given that cephalopods perform all their visual stunts with remarkably low energy expenditure. When coupled with cephalopod-like distributed sensing, power management, edge computing, and artificial intelligence for data processing and decision-making, autonomous system operation can be realized in unstructured environments with significantly improved adaptability.

## Author contributions

C. X. prepared the figures and wrote the manuscript.

## Conflicts of interest

The authors declare no competing interests.

## Data availability

No primary research results, software, or code have been included, and no new data were generated or analyzed as part of this review.

## Acknowledgements

This work was supported by the start-up funding from the University of Alabama at Birmingham.

## References

- 1 in *The Mollusca: Form and Function*, ed. K. M. Wilbur, E. R. Trueman and M. R. Clarke, Academic Press, 1985.
- 2 R. T. Hanlon, M. Vecchione and L. Allcock, *Octopus, Squid, and Cuttlefish: A Visual, Scientific Guide to the Oceans' Most*



*Advanced Invertebrates*, University of Chicago Press, 1st edn, 2018.

3 R. T. Hanlon and J. B. Messenger, *Cephalopod Behavior*, Cambridge University Press, 2nd edn, 2018.

4 W. B. Saunders and N. H. Landman, *Nautilus: the biology and paleobiology of a living fossil*, Springer, New York, 2010.

5 P. D. Ward and W. B. Saunders, Allonautilus: a new genus of living nautiloid cephalopod and its bearing on phylogeny of the Nautilida, *J. Paleontol.*, 1997, **71**, 1054–1064.

6 Anonymous, *Classic of Mountains and Seas* (c. 2000 BCE).

7 Aristotle, *History of Animals* (c. 350 BCE).

8 D'Arcy Thompson, Hectocotyle Arm – a page of Aristotle's History of Animals (1910), (available at [https://commons.wikimedia.org/wiki/File:Hectocotyle\\_Arm\\_-\\_a\\_page\\_of\\_Aristotle%27s\\_History\\_of\\_Animals\\_%28D%27Arcy\\_Thompson%29.jpg](https://commons.wikimedia.org/wiki/File:Hectocotyle_Arm_-_a_page_of_Aristotle%27s_History_of_Animals_%28D%27Arcy_Thompson%29.jpg)).

9 E. Smedley, H. J. Rose and H. J. Rose, *Encyclopaedia Metropolitana, Or, Universal Dictionary of Knowledge*, William Clowes and Sons, London, 1845.

10 P. D. de Montfort, Colossal octopus, 1810, (available at [https://commons.wikimedia.org/wiki/File:Colossal\\_octopus\\_by\\_Pierre\\_Denys\\_de\\_Montfort.jpg](https://commons.wikimedia.org/wiki/File:Colossal_octopus_by_Pierre_Denys_de_Montfort.jpg)).

11 J. Verne, *Twenty Thousand Leagues under the Sea*, Pierre-Jules Hetzel, 1870.

12 A. de Neuville and E. Riou, *Engraving of Captain Nemo viewing a giant squid from a porthole of the Nautilus submarine*, 1870, (available at <https://commons.wikimedia.org/wiki/File:20000-3.jpg>).

13 W. Sauber, Oktopusvase, 2009, (available at [https://commons.wikimedia.org/wiki/File:AMI\\_-\\_Oktopusvase.jpg](https://commons.wikimedia.org/wiki/File:AMI_-_Oktopusvase.jpg)).

14 G. Arcimboldo, *The Allegory of Water*, 1566), (available at [https://commons.wikimedia.org/wiki/File:Arcimboldo\\_water.jpg](https://commons.wikimedia.org/wiki/File:Arcimboldo_water.jpg)).

15 J. Dzik, Origin of the Cephalopoda, *Acta Palaeontol. Pol.*, 1981, **26**, 161–191.

16 B. Kröger, J. Vinther and D. Fuchs, Cephalopod origin and evolution: a congruent picture emerging from fossils, development and molecules, *BioEssays*, 2011, **33**, 602–613.

17 in *Squid as Experimental Animals*, ed. W. J. J. Adelman, J. M. Arnold and D. L. Gilbert, Springer, 1990.

18 E. Vidal, *Advances in Cephalopod Science: Biology, Ecology, Cultivation and Fisheries*, Academic Press, 2014.

19 R. Rosa, C. P. Santos, F. Borges, P. Amodio, M. Amor, J. R. Bower, R. L. Caldwell, A. Di Cosmo, M. Court, G. Fiorito, C. Gestal, Á. F. González, Á. Guerra, R. T. Hanlon, J. K. K. Hofmeister, C. M. Ibáñez, Y. Ikeda, P. Imperadore, J. G. Kommritz, M. Kuba, K. C. Hall, Z. Lajbner, T. S. Leite, V. M. Lopes, U. Markaida, N. A. Moltschanivskij, J. Nabhitabhata, N. Ortiz, E. Otjacques, F. Pizzulli, G. Ponte, G. Polese, F. Raffini, C. Rosas, Á. Roura, E. Sampaio, S. Segawa, O. Simakov, I. Sobrino, L. P. Storero, J. R. Voight, B. L. Williams, X. Zheng, G. J. Pierce, R. Villanueva and I. G. Gleadall, Past, present, and future trends in octopus research, *Octopus Biology and Ecology*, Elsevier, 2024, pp. 421–454, <https://linkinghub.elsevier.com/retrieve/pii/B9780128206393000108>.

20 J. Z. Young, Cephalopods and neuroscience, *Biol. Bull.*, 1985, **168**, 153–158.

21 R. Kautz, D. D. Ordinario, V. Tyagi, P. Patel, T. N. Nguyen and A. A. Gorodetsky, Cephalopod-Derived Biopolymers for Ionic and Protonic Transistors, *Adv. Mater.*, 2018, **30**, 1704917.

22 R. Nakajima, S. Shigeno, L. Zullo, F. De Sio and M. R. Schmidt, Cephalopods Between Science, Art, and Engineering: A Contemporary Synthesis, *Front. Commun.*, 2018, **3**, 161–191.

23 T. H. Bullock, *The Nervous Systems of Invertebrates: An Evolutionary and Comparative Approach*, Birkhäuser, Basel, 1995.

24 M. Nixon and J. Z. Young, *The Brains and Lives of Cephalopods*, Oxford University Press, 2003.

25 in *The Biology of Chameleons*, ed. K. A. Tolley and A. Herrel, University of California Press, 2013.

26 R. W. Matthews and J. R. Matthews, *Insect Behavior*, Springer, 2nd edn, 2009.

27 C.-K. Kang, J.-Y. Moon, S.-I. Lee and P. G. Jablonski, Camouflage through an active choice of a resting spot and body orientation in moths, *J. Evol. Biol.*, 2012, **25**, 1695–1702.

28 H. Steenfeldt, Amazing squid changing color, 2012, (available at <https://www.youtube.com/watch?v=OauXCp8l3QI>).

29 R. A. Cloney and S. L. Brocco, Chromatophore Organs, Reflector Cells, Iridocytes and Leucophores in Cephalopods, *Am. Zool.*, 1983, **23**, 581–592.

30 L. M. Mäthger and R. T. Hanlon, Malleable skin coloration in cephalopods: selective reflectance, transmission and absorbance of light by chromatophores and iridophores, *Cell Tissue Res.*, 2007, **329**, 179–186.

31 J. B. Messenger, Cephalopod chromatophores: neurobiology and natural history, *Biol. Rev. Cambridge Philos. Soc.*, 2001, **76**, 473–528.

32 L. M. Mäthger, E. J. Denton, N. J. Marshall and R. T. Hanlon, Mechanisms and behavioural functions of structural coloration in cephalopods, *J. R. Soc., Interface*, 2009, **6**, S149–S163.

33 R. T. Hanlon, L. M. Mäthger, G. R. R. Bell, A. M. Kuzirian and S. L. Senft, White reflection from cuttlefish skin leucophores, *Bioinspiration Biomimetics*, 2018, **13**, 035002.

34 J. Tuszyński, Invertebrates in Smithsonian National Zoological Park: *Sepia officinalis* Common Cuttlefish, 2009, (available at [https://commons.wikimedia.org/wiki/File:Washington\\_DC\\_Zoo\\_-\\_Sepia\\_officinalis\\_2.jpg](https://commons.wikimedia.org/wiki/File:Washington_DC_Zoo_-_Sepia_officinalis_2.jpg)).

35 R. T. Hanlon, A close-up of skin from the common cuttlefish (*Sepia officinalis*), 2016, (available at <https://www.sciencefriday.com/articles/secrets-of-cephalopod-camouflage/>).

36 G. Fiorito, L. Borrelli and F. Gherardi, *A Catalogue of Body Patterning in Cephalopoda*, Firenze University Press, 2006.

37 R. Hanlon, Cephalopod dynamic camouflage, *Curr. Biol.*, 2007, **17**, R400–R404.

38 R. T. Hanlon, C.-C. Chiao, L. M. Mäthger, A. Barbosa, K. Buresch and C. Chubb, Cephalopod dynamic camouflage: bridging the continuum between background matching



and disruptive coloration, *Philos. Trans. R. Soc., B*, 2009, **364**, 429–437.

39 A. Barbosa, L. M. Mathger, C. Chubb, C. Florio, C.-C. Chiao and R. T. Hanlon, Disruptive coloration in cuttlefish: a visual perception mechanism that regulates ontogenetic adjustment of skin patterning, *J. Exp. Biol.*, 2007, **210**, 1139–1147.

40 J. J. Allen, L. M. Mäthger, A. Barbosa and R. T. Hanlon, Cuttlefish use visual cues to control three-dimensional skin papillae for camouflage, *J. Comp. Physiol., A*, 2009, **195**, 547–555.

41 SUBnormali Team, *Callistoctopus macropus* (2008), (available at [https://commons.wikimedia.org/wiki/File:Octopus\\_macropus.jpg](https://commons.wikimedia.org/wiki/File:Octopus_macropus.jpg)).

42 E. Drinkwater, W. L. Allen, J. A. Endler, R. T. Hanlon, G. Holmes, N. T. Homziak, C. Kang, B. C. Leavell, J. Lehtonen, K. Loeffler-Henry, J. M. Ratcliffe, C. Rowe, G. D. Ruxton, T. N. Sherratt, J. Skelhorn, C. Skopec, H. R. Smart, T. E. White, J. E. Yack, C. M. Young and K. D. L. Umbers, A synthesis of deimatic behaviour, *Biol. Rev.*, 2022, **97**, 2237–2267.

43 R. Hanlon, Reproductive Behaviors of Caribbean Reef Squid (*Sepioteuthis sepioides*), 2012, (available at <https://www.youtube.com/watch?v=YViRSgYys1o>).

44 S. Baron, Flamboyant Cuttlefish, 2010, (available at [https://commons.wikimedia.org/wiki/File:Flamboyant\\_Cuttlefish.jpg](https://commons.wikimedia.org/wiki/File:Flamboyant_Cuttlefish.jpg)).

45 S. Zylinski and S. Johnsen, Mesopelagic Cephalopods Switch between Transparency and Pigmentation to Optimize Camouflage in the Deep, *Curr. Biol.*, 2011, **21**, 1937–1941.

46 Monterey Bay Aquarium Research Institute, Glass squid changes color in front of our eyes, (available at [https://www.youtube.com/watch?v=rAZQ6Czd\\_co](https://www.youtube.com/watch?v=rAZQ6Czd_co)).

47 Monterey Bay Aquarium Research Institute, Who is this see-through alien? 2019, (available at <https://mashable.com/article/glass-squids-taonius-galiteuthis/>).

48 New Atlantis WILD, Poisonous Octopus Fight, 2014, (available at <https://www.youtube.com/watch?v=bFGMPsb0YV0>).

49 L. M. Mathger, G. R. R. Bell, A. M. Kuzirian, J. J. Allen and R. T. Hanlon, How does the blue-ringed octopus (*Hapalochlaena lunulata*) flash its blue rings?, *J. Exp. Biol.*, 2012, **215**, 3752–3757.

50 T. Bretl, Bobtail squid (*Euprymna berryi*), 2012, (available at <https://toddbrndl.com>).

51 E. Stabb, Why sequence *Vibrio fischeri*? 2010, (available at <https://jgi.doe.gov/why-sequence-vibrio-fischeri/>).

52 S. V. Nyholm and M. McFall-Ngai, The winnowing: establishing the squid–vibrio symbiosis, *Nat. Rev. Microbiol.*, 2004, **2**, 632–642.

53 M. McFall-Ngai, Hawaiian bobtail squid, *Curr. Biol.*, 2008, **18**, R1043–R1044.

54 M. J. McFall-Ngai, The Importance of Microbes in Animal Development: Lessons from the Squid–Vibrio Symbiosis, *Annu. Rev. Microbiol.*, 2014, **68**, 177–194.

55 R. Hanlon, Papillae expression for camouflage in the giant Australian cuttlefish, 2018, (available at <https://www.youtube.com/watch?v=NDfqRZYMc8Q>).

56 J. J. Allen, G. R. R. Bell, A. M. Kuzirian and R. T. Hanlon, Cuttlefish skin papilla morphology suggests a muscular hydrostatic function for rapid changeability, *J. Morphol.*, 2013, **274**, 645–656.

57 J. J. Allen, G. R. R. Bell, A. M. Kuzirian, S. S. Velankar and R. T. Hanlon, Comparative morphology of changeable skin papillae in octopus and cuttlefish, *J. Morphol.*, 2014, **275**, 371–390.

58 D. Panetta, K. Buresch and R. T. Hanlon, Dynamic masquerade with morphing three-dimensional skin in cuttlefish, *Biol. Lett.*, 2017, **13**, 20170070.

59 P. T. Gonzalez-Bellido, A. T. Scaros, R. T. Hanlon and T. J. Wardill, Neural Control of Dynamic 3-Dimensional Skin Papillae for Cuttlefish Camouflage, *iScience*, 2018, **1**, 24–34.

60 S. Childs, Thaumoctopus mimicus, 2010, (available at [https://commons.wikimedia.org/wiki/File:Mimic\\_Octopus\\_2.jpg](https://commons.wikimedia.org/wiki/File:Mimic_Octopus_2.jpg)).

61 M. D. Norman, J. Finn and T. Tregenza, Dynamic mimicry in an Indo–Malayan octopus, *Proc. R. Soc. London. Ser. B Biol. Sci.*, 2001, **268**, 1755–1758.

62 R. T. Hanlon, L.-A. Conroy and J. W. Forsythe, Mimicry and foraging behaviour of two tropical sand-flat octopus species off North Sulawesi, Indonesia, *Biol. J. Linn. Soc.*, 2007, **93**, 23–38.

63 B. Baker, Unusual Adaptations: Evolution of the Mimic Octopus, *Bioscience*, 2010, **60**, 962.

64 E. Kreit, L. M. Mäthger, R. T. Hanlon, P. B. Dennis, R. R. Naik, E. Forsythe and J. Heikenfeld, Biological versus electronic adaptive coloration: how can one inform the other?, *J. R. Soc., Interface*, 2013, **10**, 20120601.

65 Y. Hager, Different wiring for squid's iridescent and pigment displays, *J. Exp. Biol.*, 2014, **217**, 815–816.

66 M. Layne, Chromatophores, 2007, (available at <https://commons.wikimedia.org/wiki/File:Chromatophores.jpg>).

67 R. A. Cloney and E. Florey, Ultrastructure of cephalopod chromatophore organs, *Z. Med. Phys.*, 1968, **89**, 250–280.

68 L. F. Deravi, A. P. Magyar, S. P. Sheehy, G. R. R. Bell, L. M. Mäthger, S. L. Senft, T. J. Wardill, W. S. Lane, A. M. Kuzirian, R. T. Hanlon, E. L. Hu and K. K. Parker, The structure–function relationships of a natural nanoscale photonic device in cuttlefish chromatophores, *J. R. Soc., Interface*, 2014, **11**, 20130942.

69 T. L. Williams, C. W. DiBona, S. R. Dinneen, S. F. Jones Labadie, F. Chu and L. F. Deravi, Contributions of Phenoxazone-Based Pigments to the Structure and Function of Nanostructured Granules in Squid Chromatophores, *Langmuir*, 2016, **32**, 3754–3759.

70 D. Q. Bower, S. L. Senft, R. T. Hanlon and L. F. Deravi, Pigment granule architecture varies across yellow, red, and brown chromatophores in squid *Doryteuthis pealeii*, *Sci. Rep.*, 2024, **14**, 31417.

71 G. R. R. Bell, A. M. Kuzirian, S. L. Senft, L. M. Mäthger, T. J. Wardill and R. T. Hanlon, Chromatophore radial muscle fibers anchor in flexible squid skin, *Invertebr. Biol.*, 2013, **132**, 120–132.



72 Y. Kobayashi, K. Mizusawa, Y. Saito and A. Takahashi, Melanocortin Systems on Pigment Dispersion in Fish Chromatophores, *Front. Endocrinol.*, 2012, **3**, 1–6.

73 T. L. Williams, S. L. Senft, J. Yeo, F. J. Martín-Martínez, A. M. Kuzirian, C. A. Martin, C. W. DiBona, C.-T. Chen, S. R. Dinneen, H. T. Nguyen, C. M. Gomes, J. J. C. Rosenthal, M. D. MacManes, F. Chu, M. J. Buehler, R. T. Hanlon and L. F. Deravi, Dynamic pigmentary and structural coloration within cephalopod chromatophore organs, *Nat. Commun.*, 2019, **10**, 1004.

74 G. Hanlon, Atlantic Longfin Squid, (available at <https://www.the-scientist.com/cover-story/color-from-structure-39860>).

75 L. M. Mäthger and E. J. Denton, Reflective properties of iridophores and fluorescent “eyespots” in the loliginid squid *Alloteuthis subulata* and *Loligo vulgaris*, *J. Exp. Biol.*, 2001, **204**, 2103–2118.

76 A. R. Tao, D. G. DeMartini, M. Izumi, A. M. Sweeney, A. L. Holt and D. E. Morse, The role of protein assembly in dynamically tunable bio-optical tissues, *Biomaterials*, 2010, **31**, 793–801.

77 D. G. DeMartini, D. V. Krogstad and D. E. Morse, Membrane invaginations facilitate reversible water flux driving tunable iridescence in a dynamic biophotonic system, *Proc. Natl. Acad. Sci. U. S. A.*, 2013, **110**, 2552–2556.

78 T. J. Wardill, P. T. Gonzalez-Bellido, R. J. Crook and R. T. Hanlon, Neural control of tuneable skin iridescence in squid, *Philos. Trans. R. Soc., B*, 2012, **279**, 4243–4252.

79 D. E. Morse and E. Taxon, Reflectin needs its intensity amplifier: Realizing the potential of tunable structural biophotonics, *Appl. Phys. Lett.*, 2020, **117**, 220501.

80 L. M. Mäthger, S. L. Senft, M. Gao, S. Karaveli, G. R. R. Bell, R. Zia, A. M. Kuzirian, P. B. Dennis, W. J. Crookes-Goodson, R. R. Naik, G. W. Kattawar and R. T. Hanlon, Bright White Scattering from Protein Spheres in Color Changing, Flexible Cuttlefish Skin, *Adv. Funct. Mater.*, 2013, **23**, 3980–3989.

81 D. G. DeMartini, A. Ghoshal, E. Pandolfi, A. T. Weaver, M. Baum and D. E. Morse, Dynamic biophotonics: female squid exhibit sexually dimorphic tunable leucophores and iridocytes, *J. Exp. Biol.*, 2013, **216**, 3733–3741.

82 J. Song, B. Li, L. Zeng, Z. Ye, W. Wu, B. Hu and A. Mini-Review, on Reflectins, from Biochemical Properties to Bio-Inspired Applications, *IJMS*, 2022, **23**, 15679.

83 W. J. Crookes, L.-L. Ding, Q. L. Huang, J. R. Kimbell, J. Horwitz and M. J. McFall-Ngai, Reflectins: The Unusual Proteins of Squid Reflective Tissues, *Science*, 2004, **303**, 235–238.

84 A. Chatterjee, B. Norton-Baker, L. E. Bagge, P. Patel and A. A. Gorodetsky, An introduction to color-changing systems from the cephalopod protein reflectin, *Bioinspiration Biomimetics*, 2018, **13**, 045001.

85 R. M. Kramer, W. J. Crookes-Goodson and R. R. Naik, The self-organizing properties of squid reflectin protein, *Nat. Mater.*, 2007, **6**, 533–538.

86 D. G. DeMartini, M. Izumi, A. T. Weaver, E. Pandolfi and D. E. Morse, Structures, Organization, and Function of Reflectin Proteins in Dynamically Tunable Reflective Cells, *J. Biol. Chem.*, 2015, **290**, 15238–15249.

87 R. Levenson, C. Bracken, N. Bush and D. E. Morse, Cyclable Condensation and Hierarchical Assembly of Metastable Reflectin Proteins, the Drivers of Tunable Biophotonics, *J. Biol. Chem.*, 2016, **291**, 4058–4068.

88 K. L. Naughton, L. Phan, E. M. Leung, R. Kautz, Q. Lin, Y. Van Dyke, B. Marmiroli, B. Sartori, A. Arvai, S. Li, M. E. Pique, M. Naeim, J. P. Kerr, M. J. Aquino, V. A. Roberts, E. D. Getzoff, C. Zhu, S. Bernstorf and A. A. Gorodetsky, Self-Assembly of the Cephalopod Protein Reflectin, *Adv. Mater.*, 2016, **28**, 8405–8412.

89 Z. Guan, T. Cai, Z. Liu, Y. Dou, X. Hu, P. Zhang, X. Sun, H. Li, Y. Kuang, Q. Zhai, H. Ruan, X. Li, Z. Li, Q. Zhu, J. Mai, Q. Wang, L. Lai, J. Ji, H. Liu, B. Xia, T. Jiang, S.-J. Luo, H.-W. Wang and C. Xie, Origin of the Reflectin Gene and Hierarchical Assembly of Its Protein, *Curr. Biol.*, 2017, **27**, 2833–2842.e6.

90 M. J. Umerani, P. Pratakshya, A. Chatterjee, J. A. Cerna Sanchez, H. S. Kim, G. Ilc, M. Kovačić, C. Magnan, B. Marmiroli, B. Sartori, A. L. Kwansa, H. Orins, A. W. Bartlett, E. M. Leung, Z. Feng, K. L. Naughton, B. Norton-Baker, L. Phan, J. Long, A. Allevato, J. E. Leal-Cruz, Q. Lin, P. Baldi, S. Bernstorf, J. Plavec, Y. G. Yingling and A. A. Gorodetsky, Structure, self-assembly, and properties of a truncated reflectin variant, *Proc. Natl. Acad. Sci. U. S. A.*, 2020, **117**, 32891–32901.

91 C. Xu, N. Kandel, X. Qiao, Md. I. Khan, P. Pratakshya, N. E. Tolouei, B. Chen and A. A. Gorodetsky, Long-Range Proton Transport in Films from a Reflectin-Derived Peptide, *ACS Appl. Mater. Interfaces*, 2021, **13**, 20938–20946.

92 D. D. Ordinario, L. Phan, W. G. Walkup Iv, J.-M. Jocson, E. Karshalev, N. Hüskens and A. A. Gorodetsky, Bulk protonic conductivity in a cephalopod structural protein, *Nat. Chem.*, 2014, **6**, 596–602.

93 G. Qin, P. B. Dennis, Y. Zhang, X. Hu, J. E. Bressner, Z. Sun, W. J. Crookes-Goodson, R. R. Naik, F. G. Omenetto and D. L. Kaplan, Recombinant reflectin-based optical materials, *J. Polym. Sci., Part B: Polym. Phys.*, 2013, **51**, 254–264.

94 P. B. Dennis, K. M. Singh, M. C. Vasudev, R. R. Naik and W. J. Crookes-Goodson, Research Update: A minimal region of squid reflectin for vapor-induced light scattering, *APL Mater.*, 2017, **5**, 120701.

95 T. Cai, K. Han, P. Yang, Z. Zhu, M. Jiang, Y. Huang and C. Xie, Reconstruction of Dynamic and Reversible Color Change using Reflectin Protein, *Sci. Rep.*, 2019, **9**, 5201.

96 L. Phan, W. G. Walkup, D. D. Ordinario, E. Karshalev, J. Jocson, A. M. Burke and A. A. Gorodetsky, Reconfigurable Infrared Camouflage Coatings from a Cephalopod Protein, *Adv. Mater.*, 2013, **25**, 5621–5625.

97 L. Phan, D. D. Ordinario, E. Karshalev, W. G. Walkup Iv, M. A. Shenk and A. A. Gorodetsky, Infrared invisibility stickers inspired by cephalopods, *J. Mater. Chem. C*, 2015, **3**, 6493–6498.

98 J. J. Loke, S. Hoon and A. Miserez, Cephalopod-Mimetic Tunable Photonic Coatings Assembled from Quasi-Mono-dispersed Reflectin Protein Nanoparticles, *ACS Appl. Mater. Interfaces*, 2022, **14**, 21436–21452.



99 D. D. Ordinario, E. M. Leung, L. Phan, R. Kautz, W. K. Lee, M. Naeim, J. P. Kerr, M. J. Aquino, P. E. Sheehan and A. A. Gorodetsky, Protochromic Devices from a Cephalopod Structural Protein, *Adv. Opt. Mater.*, 2017, **5**, 1600751.

100 Y.-C. Lin, E. Masquelier, Y. Al Sabeh, L. Sepunaru, M. J. Gordon and D. E. Morse, Voltage-calibrated, finely tunable protein assembly, *J. R. Soc., Interface*, 2023, **20**, 20230183.

101 Y. Lin, C. Yang, S. Tochikura, J. R. Uzarski, D. E. Morse, L. Sepunaru and M. J. Gordon, Electrochemically Driven Optical Dynamics of Reflectin Protein Films, *Adv. Mater.*, 2025, **37**, 2411005.

102 E. Wolde-Michael, A. D. Roberts, D. J. Heyes, A. G. Dumanli, J. J. Blaker, E. Takano and N. S. Scrutton, Design and fabrication of recombinant reflectin-based multilayer reflectors: bio-design engineering and photoisomerism induced wavelength modulation, *Sci. Rep.*, 2021, **11**, 14580.

103 C. M. Tobin, R. Gordon, S. K. Tochikura, B. F. Chmelka, D. E. Morse and J. Read De Alaniz, Reversible and size-controlled assembly of reflectin proteins using a charged azobenzene photoswitch, *Chem. Sci.*, 2024, **15**, 13279–13289.

104 A. Chatterjee, J. A. Cerna Sanchez, T. Yamauchi, V. Taupin, J. Couvrette and A. A. Gorodetsky, Cephalopod-inspired optical engineering of human cells, *Nat. Commun.*, 2020, **11**, 2708.

105 G. Bogdanov, A. Chatterjee, N. Makeeva, A. Farrukh and A. A. Gorodetsky, Squid leucophore-inspired engineering of optically dynamic human cells, *iScience*, 2023, **26**, 106854.

106 S. R. Dinneen, R. M. Osgood, M. E. Greenslade and L. F. Deravi, Color Richness in Cephalopod Chromatophores Originating from High Refractive Index Biomolecules, *J. Phys. Chem. Lett.*, 2017, **8**, 313–317.

107 F. Figon, T. Munsch, C. Croix, M.-C. Viaud-Massuard, A. Lanoue and J. Casas, Uncyclized xanthommatin is a key ommochrome intermediate in invertebrate coloration, *Insect Biochem. Mol. Biol.*, 2020, **124**, 103403.

108 L. F. Deravi, I. Cui and C. A. Martin, Using cephalopod-inspired chemistry to extend long-wavelength ultraviolet and visible light protection of mineral sunscreens, *Int. J. Cosmet. Sci.*, 2024, **46**, 941–948.

109 L. F. Deravi, N. C. Cox and C. A. Martin, Evaluation of Biologically Inspired Ammonium Xanthommatin as a Multifunctional Cosmetic Ingredient, *JID Innovations*, 2022, **2**, 100081.

110 C. A. Martin, M. Rezaeeyazdi, T. Colombani, S. R. Dinneen, A. Kumar, S. A. Bencherif and L. F. Deravi, A bioinspired, photostable UV-filter that protects mammalian cells against UV-induced cellular damage, *Chem. Commun.*, 2019, **55**, 12036–12039.

111 Z. Lin, Z. Gong, D. Q. Bower, D. Lee and L. F. Deravi, Bidispersed Colloidal Assemblies Containing Xanthommatin Produce Angle-Independent Photonic Structures, *Adv. Opt. Mater.*, 2021, **9**, 2100416.

112 J.-H. Kim, J.-Y. Lee, J. Kim, Z. Gong, D. J. Wilson, L. F. Deravi and D. Lee, Adaptive coloration enabled by the reversible osmotic annealing of chromatophore-like microcapsules, *J. Mater. Chem. C*, 2024, **12**, 2148–2155.

113 C. A. Martin, Z. Lin, A. Kumar, S. R. Dinneen, R. M. Osgood and L. F. Deravi, Biomimetic Colorants and Coatings Designed with Cephalopod-Inspired Nanocomposites, *ACS Appl. Bio Mater.*, 2021, **4**, 507–513.

114 C. L. Martin, K. R. Flynn, T. Kim, S. K. Nikolic, L. F. Deravi and D. J. Wilson, Color-Changing Paints Enabled by Photoresponsive Combinations of Bio-Inspired Colorants and Semiconductors, *Adv. Sci.*, 2023, **10**, 2302652.

115 A. Kumar, T. L. Williams, C. A. Martin, A. M. Figueiroa-Navedo and L. F. Deravi, Xanthommatin-Based Electrochromic Displays Inspired by Nature, *ACS Appl. Mater. Interfaces*, 2018, **10**, 43177–43183.

116 P. A. Sullivan, D. J. Wilson, M. Vallon, D. Q. Bower and L. F. Deravi, Inkjet Printing Bio-Inspired Electrochromic Pixels, *Adv. Mater. Interfaces*, 2023, **10**, 2202463.

117 J.-Y. Lee, J. Kim, L. F. Deravi and D. Lee, Reversible Electrophoretic Control of Structural Color Using Polymer-Stabilized, Pigment-Impregnated Colloidal Particles, *ACS Appl. Mater. Interfaces*, 2025, **17**, 22035–22041.

118 D. J. Wilson, F. J. Martín-Martínez and L. F. Deravi, Wearable Light Sensors Based on Unique Features of a Natural Biochrome, *ACS Sens.*, 2022, **7**, 523–533.

119 S.-Y. Lee and S.-J. Park, TiO<sub>2</sub> photocatalyst for water treatment applications, *J. Ind. Eng. Chem.*, 2013, **19**, 1761–1769.

120 I. H. Ifijen and S. I. Omonmhenle, Polystyrene-Based Photonic Crystals with Chemical, Thermal, and Bio-Responsive Properties, *Biomed. Mater. Devices*, 2024, **2**, 168–177.

121 C. Yu, Y. Li, X. Zhang, X. Huang, V. Malyarchuk, S. Wang, Y. Shi, L. Gao, Y. Su, Y. Zhang, H. Xu, R. T. Hanlon, Y. Huang and J. A. Rogers, Adaptive optoelectronic camouflage systems with designs inspired by cephalopod skins, *Proc. Natl. Acad. Sci. U. S. A.*, 2014, **111**, 12998–13003.

122 D. Kim, S. W. Seon, M. Shin, J. Kim, B. Kim, J. Joo, S. U. Park, W. Kim, H. K. Lee, B. W. Lee, S. G. Lee, S. E. Lee, J.-H. Seo, S. H. Han, B. H. Kim and S. M. Won, Squid-inspired and wirelessly controllable display for active camouflage in aquatic-environment, *npj Flex Electron.*, 2024, **8**, 7.

123 Y. Yu, X. Zhu, S. Jiang, S. Wu, Y. Zhao, L. Zhang, L. Song and Y. Huang, Cephalopods' Skin-Inspired Design of Nanoscale Electronic Transport Layers for Adaptive Electrochromic Tuning, *Adv. Sci.*, 2024, **11**, 2405444.

124 J. Zhou, Z. Teng, Z. Han, K. Wang, J. Hu, Y. Li, S. Wang and Y. Xia, Artificial Cephalopod Skins with Switchable Appearance Color, *Macromol. Rapid Commun.*, 2025, **46**, 2400937.

125 D. Han, Y. Wang, C. Yang and H. Lee, Multimaterial Printing for Cephalopod-Inspired Light-Responsive Artificial Chromatophores, *ACS Appl. Mater. Interfaces*, 2021, **13**, 12735–12745.

126 S. A. Morin, R. F. Shepherd, S. W. Kwok, A. A. Stokes, A. Nemiroski and G. M. Whitesides, Camouflage and Display for Soft Machines, *Science*, 2012, **337**, 828–832.

127 Q. Wang, G. R. Gossweiler, S. L. Craig and X. Zhao, Cephalopod-inspired design of electro-mechano-chemically responsive



elastomers for on-demand fluorescent patterning, *Nat. Commun.*, 2014, **5**, 4899.

128 Q. Guo, B. Huang, C. Lu, T. Zhou, G. Su, L. Jia and X. Zhang, A cephalopod-inspired mechanoluminescence material with skin-like self-healing and sensing properties, *Mater. Horiz.*, 2019, **6**, 996–1004.

129 C. Larson, B. Peele, S. Li, S. Robinson, M. Totaro, L. Beccai, B. Mazzolai and R. Shepherd, Highly stretchable electroluminescent skin for optical signaling and tactile sensing, *Science*, 2016, **351**, 1071–1074.

130 H. Shi, S. Wu, M. Si, S. Wei, G. Lin, H. Liu, W. Xie, W. Lu and T. Chen, Cephalopod-Inspired Design of Photomechanically Modulated Display Systems for On-Demand Fluorescent Patterning, *Adv. Mater.*, 2022, **34**, 2107452.

131 C. Xu, G. T. Stiubianu and A. A. Gorodetsky, Adaptive infrared-reflecting systems inspired by cephalopods, *Science*, 2018, **359**, 1495–1500.

132 Y. Liu, Z. Feng, C. Xu, A. Chatterjee and A. A. Gorodetsky, Reconfigurable Micro- and Nano-Structured Camouflage Surfaces Inspired by Cephalopods, *ACS Nano*, 2021, **15**, 17299–17309.

133 B. Yao, X. Xu, Z. Han, W. Xu, G. Yang, J. Guo, G. Li, Q. Wang and H. Wang, Cephalopod-inspired polymer composites with mechanically tunable infrared properties, *Sci. Bull.*, 2023, **68**, 2962–2972.

134 E. M. Leung, M. Colorado Escobar, G. T. Stiubianu, S. R. Jim, A. L. Vyatskikh, Z. Feng, N. Garner, P. Patel, K. L. Naughton, M. Follador, E. Karshalev, M. D. Trexler and A. A. Gorodetsky, A dynamic thermoregulatory material inspired by squid skin, *Nat. Commun.*, 2019, **10**, 1947.

135 M. A. Badshah, E. M. Leung, P. Liu, A. A. Strzelecka and A. A. Gorodetsky, Scalable manufacturing of sustainable packaging materials with tunable thermoregulability, *Nat. Sustain.*, 2022, **5**, 434–443.

136 C. Xu, M. Colorado Escobar and A. A. Gorodetsky, Stretchable Cephalopod-Inspired Multimodal Camouflage Systems, *Adv. Mater.*, 2020, **32**, 1905717.

137 P. Pratakshya, C. Xu, D. J. Dibble, A. Mukazhanova, P. Liu, A. M. Burke, R. Kurakake, R. Lopez, P. R. Dennison, S. Sharifzadeh and A. A. Gorodetsky, Octopus-inspired deception and signaling systems from an exceptionally-stable acene variant, *Nat. Commun.*, 2023, **14**, 8528.

138 J. H. Pikul, S. Li, H. Bai, R. T. Hanlon, I. Cohen and R. F. Shepherd, Stretchable surfaces with programmable 3D texture morphing for synthetic camouflaging skins, *Science*, 2017, **358**, 210–214.

139 F. Fei, P. Kotak, L. He, X. Li, C. Vanderhoef, C. Lamuta and X. Song, Cephalopod-Inspired Stretchable Self-Morphing Skin Via Embedded Printing and Twisted Spiral Artificial Muscles, *Adv. Funct. Mater.*, 2021, **31**, 2105528.

140 S. Kim, E. Eig and B. Tian, The convergence of bioelectronics and engineered living materials, *Cell Rep. Phys. Sci.*, 2024, **5**, 102149.

141 J. Liu, *et al.*, Genetically targeted chemical assembly of functional materials in living cells, tissues, and animals, *Science*, 2020, **367**, 1372–1376.

